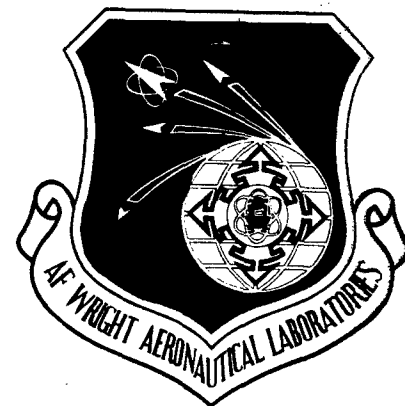


AFWAL-TR-83-4064

ADA133050

SPECTROSCOPIC CHARACTERIZATION OF THE CURED STATE OF
ACETYLENE-TERMINATED RESIN



J. L. Koenig
Case Western Reserve University
Cleveland, Ohio 44106

August 1983

Final Report for Period March 1982 to March 1983

Approved for public release; distribution unlimited

Best Available Copy

MATERIALS LABORATORY
AIR FORCE WRIGHT AERONAUTICAL LABORATORIES
AIR FORCE SYSTEMS COMMAND
WRIGHT-PATTERSON AIR FORCE BASE, OHIO 45433

20040219060

NOTICE

When Government drawings, specifications, or other data are used for any purpose other than in connection with a definitely related Government procurement operation, the United States Government thereby incurs no responsibility nor any obligation whatsoever; and the fact that the Government may have formulated, furnished, or in any way supplied the said drawings, specifications, or other data, is not to be regarded by implication or otherwise as in any manner licensing the holder or any other person or corporation, or conveying any rights or permission to manufacture, use, or sell any patented invention that may in any way be related thereto.

This report has been reviewed by the Office of Public Affairs (ASD/PA) and is releasable to the National Technical Information Service (NTIS). At NTIS, it will be available to the general public, including foreign nations.

This technical report has been reviewed and is approved for publication.



CHARLES Y-C. LEE
Project Scientist



R. L. VAN DEUSEN
Chief, Polymer Branch
Nonmetallic Materials Division

FOR THE COMMANDER



FRANKLIN D. CHERRY, Chief
Nonmetallic Materials Division

"If your address has changed, if you wish to be removed from our mailing list, or if the addressee is no longer employed by your organization please notify AFWAL/MLBP, W-PAFB, Ohio 45433 to help us maintain a current mailing list.

Copies of this report should not be returned unless return is required by security considerations, contractual obligations, or notice on a specific document.

Unclassified

SECURITY CLASSIFICATION OF THIS PAGE (When Data Entered)

REPORT DOCUMENTATION PAGE		READ INSTRUCTIONS BEFORE COMPLETING FORM
1. REPORT NUMBER AFWAL-TR-83-4064	2. GOVT ACCESSION NO.	3. RECIPIENT'S CATALOG NUMBER
4. TITLE (and Subtitle) SPECTROSCOPIC CHARACTERIZATION OF THE CURED STATE OF ACETYLENE-TERMINATED RESIN	5. TYPE OF REPORT & PERIOD COVERED Final Report March 1982-March 1983	
	6. PERFORMING ORG. REPORT NUMBER	
7. AUTHOR(s) Jack L. Koenig Department of Macromolecular Science Case Western Reserve University, Cleveland, OH	8. CONTRACT OR GRANT NUMBER(s) F33615-82-K-5038	
9. PERFORMING ORGANIZATION NAME AND ADDRESS Case Western Reserve University Cleveland, Ohio 44106	10. PROGRAM ELEMENT, PROJECT, TASK AREA & WORK UNIT NUMBERS 61101F/ILIR/01/ILIRO151	
11. CONTROLLING OFFICE NAME AND ADDRESS AFWAL/MLBP Wright-Patterson AFB, Ohio 45433	12. REPORT DATE August 1983	
	13. NUMBER OF PAGES 70	
14. MONITORING AGENCY NAME & ADDRESS (if different from Controlling Office)	15. SECURITY CLASS. (of this report) Unclassified	
	15a. DECLASSIFICATION/DOWNGRADING SCHEDULE	
16. DISTRIBUTION STATEMENT (of this Report) Approved for public release; distribution unlimited		
17. DISTRIBUTION STATEMENT (of the abstract entered in Block 20, if different from Report)		
18. SUPPLEMENTARY NOTES		
19. KEY WORDS (Continue on reverse side if necessary and identify by block number) Acetylene-terminated sulfone FTIR Solid State NMR Cure Mechanism		
20. ABSTRACT (Continue on reverse side if necessary and identify by block number) The acetylene-terminated resin, bis 4-(3-ethynylphenoxy)phenyl sulfone (AT) has been studied using Fourier transform infrared spectroscopy (FT-IR) and high resolution nuclear magnetic resonance spectroscopy of solids. Samples which were cured at different temperatures for various times were analyzed by FT-IR and the results interpreted using factor analysis. The analysis revealed that only two major components were involved in the curing mechanism, that is, only a single polymerization reaction occurred at low curing temperatures. The (CONTINUED)		

DD FORM 1473 EDITION OF 1 NOV 65 IS OBSOLETE

Unclassified

SECURITY CLASSIFICATION OF THIS PAGE (When Data Entered)

(BLOCK 20 CONTINUED)

pure component spectra generated by the factor analysis procedure could be used to analyze the state of cure of the resin. The infrared spectrum of the polymer is consistent with a polydiene structure.

The NMR results produced a similar structural result. The extent of cure of the AT resin as evidenced by the disappearance of the acetylene carbon followed a similar path to the infrared results. The inherent broadness of the carbon resonances indicates a substantial change in the molecular mobility or the existence of several structurally distinct carbons. The FT-IR results indicate the formation of only a single structure so the broadness reflects either the existence of very short oligomeric species or decreased molecular motion. It is felt that both line broadening mechanisms are occurring. Using the variable pulse sequences available to vary the extent of the dipolar coupling, it is possible to monitor the changes in carbon types as the cure parameters are varied. The new resonances appear in the 110-150ppm region of the spectrum and the changes correspond precisely to those predicted from the conjugated polyene structure in either the linear conformation or the trisubstituted benzene structure.

Curve studies also focussed on the effect of high temperature post cures of the ATS resin. Structural changes were reflected by spectroscopic differences but the changes were small and precise assignments were not possible. Further model compound studies would allow a precise determination of the structural basis of these spectroscopic differences.

FORWARD

This report on "Spectroscopic Characterization of the Cured State of Acetylene-Terminated Resin", was prepared in the Department of Macromolecular Science, Case Western Reserve University, Cleveland, Ohio 44106, under contract F33615-82-K-5038 (Project ILIR0151). It was administered under the direction of the Materials Laboratory, Air Force Wright Aeronautical Laboratories, Wright-Patterson Air Force Base, Ohio, by Dr. C. Y-C. Lee.

This report covers work conducted from 1 April 1982 to 31 March 1983. It was submitted in May 1983. The author and principal investigator of this report is Professor Jack L. Koenig.

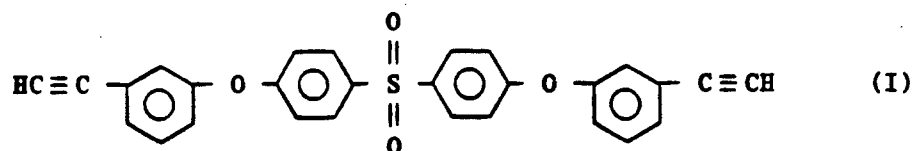
TABLE OF CONTENTS

SECTION	PAGE
I. INTRODUCTION	1
II. CARBON-13 NMR RESULTS	3
III. FTIR RESULTS	16
IV. LIST OF TABLES	26
V. LIST OF ILLUSTRATIONS	27
VI. TABLES	30
VII. ILLUSTRATIONS	35

SECTION I

Acetylene-terminated (AT) resins have been proposed as coatings, adhesives, and composite matrices, especially where stability at high temperatures is a requirement. Polymerization occurs by free-radical addition through the acetylenic moiety, and when initiated thermally, results in the extension, rigidizing, and crosslinking of the polymer. An important advantage of these systems is that thermal polymerization will occur without the formation and evolution of volatile by-products and therefore eliminates the adverse mechanical effects of voiding within the cured matrix.

The AT resin, bis[4-(3-ethynylphenoxy)phenyl] sulfone (I), has been studied in an effort to elucidate possible mechanisms of thermal cure.



It has been proposed that spectroscopic characterization of the state of cure be utilized as a tool to detect the disappearance of the acetylenic functional groups and the appearance of reaction products.

One major complicating factor in the characterization of AT resins is that even at partial cures, the material is intractable, so that ordinary methods of analysis involving dissolution cannot be used. Another factor is that the initially small concentration of acetylenic functional groups requires extremely sensitive techniques to follow reaction mechanisms. It is proposed that carbon-13 nuclear magnetic resonance (^{13}C NMR) and Fourier transform infrared (FTIR) spectroscopic techniques satisfy these experimental requirements, and will provide cure state parameters that are unique functions of mechanical properties.

SECTION II

Carbon-13 NMR spectroscopy is a useful technique for the chemical characterization of solid polymers. ^{13}C NMR allows structural group identification and is structure specific. These capabilities have been shown to be useful in the characterization of the complex networks formed in crosslinked polymer systems, and should therefore be useful in the characterization of cured ATS resins. The major reason for ^{13}C NMR's recent popularity as an analytical tool for solids was the development of the techniques of high power heteronuclear decoupling, cross-polarization, and magic angle sample spinning (MASS). These techniques have therefore been applied to the analysis of ATS resin in the monomeric, cured, and postcured states in order to elucidate mechanisms of thermal polymerization.

Unfortunately, a number of problems were anticipated as ^{13}C NMR was used in the analysis of ATS resins. First, a very large number of signals are required to be averaged in order to achieve an adequate signal-to-noise ratio. This is due mainly to the fact that there are a large number of initially diverse carbon types which reduces the signal of each particular carbon for a given sample volume. Other difficulties arise from use of the MASS technique. Because of the rapid spinning rates required to average chemical shift anisotropy and, to reduce spinning sideband contributions to the spectrum, rotors have been machined

out of polyoxymethylene (Delrin). Delrin is a tough material capable of achieving 3.5 - 4.0 KHz spinning rates. However, a very strong resonance results from the Delrin carbons appearing at 89 ppm. This resonance obscurs the resolution of the acetylene carbons in ATS resin which appear at 82 ppm. Rotors machined from another material, Kel-F, although they do not contribute any resonance to the ^{13}C NMR spectrum, only attain spinning rates of 2.0 - 2.5 KHz. This slower spinning rate creates interferences due to spinning sidebands. Figure 1 illustrates the difference in the spectra of ATS monomer when Delrin and Kel-F rotors are used for sample spinning. Using the Kel-F rotor, the acetylene resonances are free from Delrin overlap and can be quantitatively measured for analysis of acetylenic loss. However, because of the slower maximum spinning rates of the Kel-F rotors, spinning sidebands are greater in number and intensity and spinning rates must be chosen so as to minimize interference with principle bands. Interference is more difficult to work around after curing has occurred and resonances broaden. Furthermore, the area under these sidebands must be considered when using peak areas for quantitative analysis. Finally, the most serious of the difficulties encountered is the significant line broadening of the carbon resonances upon curing of the ATS resin. Line broadening, which decreases resolution, results from many contributions. The line broadening that occurs in this system is expected, however, to be due, for the most part, to the structural diversity of network that is formed upon

cure. Structurally distinct carbons giving rise to new resonances at slightly different frequencies will, therefore, result in overlapping lines that are not resolved by MASS. This creates difficulties in distinguishing and assigning new peaks and in many cases excludes the possibility of quantitative analysis.

Carbon-13 NMR spectra were recorded with a Nicolet Technology NT-150 spectrometer equipped with a cross-polarization accessory. Radio frequency amplifiers provided approximately 350 watts at 150.0 MHz and approximately 750 watts at 37.7 MHz, and were adjusted to satisfy the Hartmann-Hahn condition at roughly 58 KHz. The cross-polarization experiment was conducted with a contact time of 1.0 msec and with a delay of 2.0 seconds between pulse sequence repetitions. Samples were spun at the magic angle (54.7 degrees) in Beams-Andrew type rotors machined from Delrin and Kel-F rods. Delrin rotors typically achieved speeds of 3.5 KHz, while for Kel-F rotors 2.5 KHz was attained. The magic angle was set by maximizing the intensity of the carbonyl resonance of glycine. The resonance from the Delrin rotors (89 ppm downfield from tetramethylsilane) was used for reference. Approximately 20,000 transients were collected for each sample which were then block averaged using maximum analog-to-digital conversion in order to gain sensitivity.

Shown in figure 2a is the cross-polarization spectrum of the ATS monomer. Even though the resin in its uncured state is soluble, it is useful for purposes of comparison to obtain the solid state spectrum of the material. The spectrum of the monomer exhibits resolution sufficient to assign resonances to each of the chemically distinct carbons contained in the monomer structure. A dipolar dephasing pulse sequence was utilized in distinguishing the five quaternary carbons shown in figure 2b. Assignments were made for the remaining aromatic carbons based on intensity considerations and on additivity rules of chemical shifts for substituted benzene. Chemical shifts were calculated based on constants for a terminal ethynyl group and a phenoxy group on a meta-substituted benzene ring. The observed and calculated chemical shifts are listed in table 1. For most carbons, assignments correspond to those made previously from solution studies. Peaks at 164 ppm and 154 ppm are due to the two aryl ether carbons. The peaks from 140-120 ppm arise from the remaining aromatic carbons. Both acetylenic carbons exhibit resonances at approximately 82 ppm. These resonances are overlapped and appear as a single resonance. Use of the dipolar dephasing pulse sequence allowed selective suppression of the protonated terminal acetylene carbon, thus distinguishing it as the slightly higher field resonance.

Additionally, this pulse sequence has led to the tentative reassignment of the resonances in the 127-115 ppm region. Previous work has assigned the resonances at 116.5 ppm to carbons (j) (two chemically equivalent carbons); 121.4 ppm to carbon (g); 125.4 ppm to carbon (d); and 126.5 ppm to carbon (c). It should be noted, however, that the resonance at 125.4 ppm is approximately twice as intense as the other resonances in the region; indicating two carbons instead of one. When this peak was deconvoluted from the peak at 126.5 ppm, the area was confirmed to be twice that of the other resonances. When the peak was examined more closely, a shoulder was apparent on the high field side. Furthermore, the dipolar dephasing pulse sequence suppressed all resonances in the immediate region except for the peak at 125.4 ppm - the downfield side of the double band. This resonance must therefore be assigned to carbon (c) as it is the only quaternary carbon of those in question. The assumption was then made that the two carbons represented by carbon (j) actually have inequivalent resonances. Because the separation of these two resonances is expected to be rather small, it is quite likely that they appear at 126.5 ppm and the shoulder at 125.0 ppm. The resonances at 121.4 ppm and 116.5 ppm must then represent carbons (d) and (g) respectively. The assignment is considered tentative because of the discrepancy between the calculated and assigned values for the resonances of the (j) carbons. It is interesting to note that the resonance at 131.0 ppm which is assigned to both (k) carbons (also twice the

intensity), when resolved into its component peaks, shows resonances at 131.2 and 130.8 ppm - not nearly the splitting seen in the (j) carbons.

In order to effectively analyze the ^{13}C NMR spectra of cured ATS resins, previous work was examined and the effects of the proposed mechanisms of cure were considered. Much emphasis has been placed on the possibility of cyclotrimerization being a major contributing mechanism. Chemical shifts were calculated for the theoretical structures resulting from this mechanism; 1,2,4- and 1,3,5-trisubstituted benzene. Table 2 shows the expected changes in chemical shifts. These are possible to predict using additivity rules for substituted benzenes. However, additivity rules for other possible structures have not been established and chemical shifts can only be predicted from those observed for similar, known structures. For the linear polyene structure, which is thought to predominate, chemical shifts corresponding to those observed for styrenes may indicate the range where resonance should be expected. For a 4-substituted styrene, the chemical shifts for the (a) and (b) carbons are reported to be 135-138 ppm and 109-116 ppm respectively. α -substituted styrenes show slightly higher resonances for the a carbon; 141.9 ppm for methyl-substituted, and 148.8 ppm for ethyl-substituted styrenes. Changes in chemical shifts for the aromatic carbons would be similar to those listed in table 2. From the above considerations it

follows that for polymerization to a polyene structure, resonances from carbons (a) and (b) would be expected to be concentrated in the regions of 135-150 ppm and 109-116 ppm respectively. Structures formed by cyclotrimerization reactions would yield these resonances at 139-142 ppm and 125-129 ppm, although this latter region should not appear significantly changed since resonances from pendant phenyl carbons (c) and (e) will disappear from this same region.

In figure 3, ^{13}C NMR spectra illustrate the effect of ATS cure at 120 C for various times. The anticipated line broadening is readily observable after 30 minutes of cure, and resolution of individual carbon signals deteriorates considerably after 60 minutes of cure. As can be seen, the acetylene resonance is still present after 12 hours of cure. In fact, FTIR measurements indicate that approximately 65% of the acetylene absorbance remains. For the first hour of cure, it appears that little more than line broadening of existing carbons occurs. By one hour of cure, new resonances in the 125-117 ppm region are evident. In figure 4, the difference spectrum between the 12 hour cure and the 1 hour cure is illustrated. Principle differences are substantial increases in the resonances around 130 ppm and also increases in the resonances from 125-115 ppm. Smaller increases occur at approximately 147 ppm and 139 ppm. No definitive assignments or interpretations can be made regarding these changes, although they seem to correlate more closely with the

changes expected from a cyclotrimerization reaction rather than from linear polyene formation.

ATS was thermally cured at higher temperatures according to different cure cycles; 1) 3 hours at 150 C; 2) 10 minutes at 300 C; and 3) 3 hrs at 150 C followed by a postcure of 10 minutes at 300 C. Based on previous work, these conditions were considered to well represent substantial low temperature cure, high temperature cure, and low, followed by high temperature postcure. Certainly, other cycles and combinations of cycles are desirable for a comprehensive study. In order to account for line broadening of the aromatic carbons, the monomer spectrum was artificially broadened to approximate the degree of broadening in the cured samples. Figure 5 illustrates the monomer with artificial line broadening and the cross-polarization spectra of ATS following the three cure cycles. The spectra are shown only for the 170-105 ppm region since no other changes are detectable. No acetylenic resonances are observed for any of the cured samples, although because of the broad Delrin resonance, complete acetylene loss was not certain. A degree-of-cure of over 97% was later confirmed by FTIR spectra of the same material. This fact contradicts earlier cure studies that were conducted for FTIR measurements. The earlier cure cycles were conducted in air; one occurred in a heating cell inside the FTIR instrument; another in a carefully monitored oil bath. The cure cycle for this NMR study was conducted in a nitrogen atmosphere in which

the pyrex tube was inserted into a well-fitted steel jacket in a muffle furnace. In this latter case, the thermocouple was not inserted into the sample directly, but rather in an equivalent position in the steel jacket. The two possible explanations, then, for the discrepancy are 1) the nitrogen atmosphere gave rise to an increased consumption of acetylene groups; this seems unlikely from other studies, or 2) the actual temperature of the polymerization was somewhat higher than recorded from the thermocouple, leading to an increased rate of reaction. The purpose of this latter cure cycle was not to obtain DOC measurements, but rather relative effects of substantially different cure cycles. Therefore, the discrepancy is not deemed to significantly affect the results or interpretation of the study.

Table 3 lists the percentage breakdown of contributions to the spectra from acetylenic, 150-110 ppm, and aryl ether carbon types. The 150-110 ppm region of the monomer spectrum includes resonances from only those carbon types that are aromatic. Because of very similar shielding effects, this region is also expected to include, if present, resonances from other carbon types such as doubly bonded carbons and carbons in conjugated systems. The data indicates the entire quantity of acetylene carbons consumed at these cure conditions result in structures that resonate in the 150-110 ppm region of the spectrum. Differences within this region, then, are expected to indicate

what, if any, differences in polymerization mechanisms occur. The slight decrease noted in the area of the aryl ether resonances is not readily explained, but may be due in part to increased mobility in the C-O bonds upon cure.

Further study was conducted on the materials cured according to the above conditions in order to determine differences in the ^{13}C NMR spectra that would distinguish more clearly the effects of curing conditions. A technique was used that utilizes the protonated carbon suppression pulse sequence to provide information on the relative percentage of quaternary and protonated carbons within the 150-110 ppm band. This dipolar dephasing sequence makes use of the significantly different transverse relaxation constants between protonated carbons ($<20 \mu\text{sec}$), and quaternary carbons ($>150 \mu\text{sec}$). This technique has been reported elsewhere for use in the study of coals. Experimental evidence has been established indicating that the carbon magnetization, which decays transversely as a function of dephasing time (T_{DD}), also decays as a function of nearest neighbor interactions. For carbons directly bonded to protons, very rapid dephasing occurs as is evidenced by a rapid decay of the signal as T_{DD} is increased. Carbons that are quaternary retain their magnetization for much longer times. This is illustrated in figure 6 for the sample cured for 10 minutes at 300 C. As can be seen, with a delay of 50 μsec , virtually all of the resonances from protonated carbons have been suppressed. The

remaining resonances are located in the range of 150-135 ppm. These resonances must be due to carbon (1), and carbons (b) and (c) after changes in their chemical shifts occur due to cure.

It has been shown that the rapid decays which results from the proton nearest neighbor dipole interactions can be well approximated by a second-order Gaussian decay; while for the quaternary carbons, a first-order or Lorentzian decay describes the longer relaxation mechanism. Figure 7 is a plot of magnetization versus dephasing delay time (T_{DD}) for the 150-110 ppm region of ATS resin cured 10 minutes at 300 C. As was described, the short decaying component was fit with a Gaussian curve and the longer component by a Lorentzian using a non-linear least-squares iteration procedure. The areas of the 150-110 ppm band (at $T_{DD} = 0$) that correspond to protonated and quaternary carbons and the corresponding T_2^* decay constants were calculated based on the following expression:

$$A(T_{DD}) = A_{o_p} \exp[-.5(T_{DD}/T_{2p}^*)^2] + A_{o_q} \exp[-T_{DD}/T_{2q}^*]$$

where $A(T_{DD})$ is the total magnetization (measured as area of the 150-110 ppm band), A_{o_p} is the area contribution of the protonated carbons at $T_{DD} = 0$, A_{o_q} is the area contribution of the quaternary carbons at $T_{DD} = 0$, and T_2^* is the transverse relaxation constant. Results are shown for the three different cured samples in table 4. The aryl ether band exhibits only the

long decay of quaternary carbon (T_2^* is approx. 300 μ sec). This result was expected and indicates that the broadening of this band is most likely due to structural changes involving the aryl ether carbons. The 150-110 ppm band, however, is made up mainly from contributions due to protonated carbons. As table 4 indicates, though, this band contains a greater percentage of quaternary carbons after cure; an increase from 22.7% to 27-28%. This indicates that of the new carbon resonances being added to the 150-110 ppm region, approximately 50% are quaternary. Therefore, we can conclude that neither proton loss nor proton gain in the acetylene carbons, occurs to any great extent upon cure.

Figure 8 illustrates the subtraction of the line broadened monomer from the ATS cured for 10 minutes at 300 C. The new resonances that appear are concentrated in the regions of 147-136 ppm and 115-110 ppm. Decreases occur in the regions of 135-129 ppm and 127-124 ppm. At this time, the changes that occur follow the trends expected from both the linear polyene polymerization mechanism and that of cyclotrimerization, and distinction between the two conformations is difficult to make. Little change is noted between the spectra of ATS cured 10 minutes at 300 C and ATS cured 3 hours at 150 C. The former appears to contain somewhat stronger resonances at 136 ppm and 129-124 ppm, again supporting a polyene structure; be it linear or cyclic. It is interesting to note that virtually no changes occur in the

spectra upon postcure of the ATS cured 3 hours at 150 C. This indicates only that rearrangement does not occur since all acetylene carbons have been consumed in the initial cure.

Some changes are apparent between ATS cured at 120 C and ATS cured at the higher temperatures. Figure 9 shows the difference spectrum between ATS cured 10 minutes at 300 C and ATS cured 12 hours at 120 C. The higher temperature cure produces broad resonances in the 148-136 ppm, 134-124 ppm, and 123-115 ppm regions, that are not found in the ATS cured at the lower temperature. Again, no conclusive assignments of these resonances are possible, but because the spectra show significant differences, further study is merited. Postcure of the low temperature cured ATS may provide additional information.

In conclusion, what we have shown, is the ability, through modifications in the NMR pulse sequence, to better monitor the changes in carbon types as the cure parameters are varied. Our data shows that as the acetylene resonances disappear, new resonances are seen in the 150-110 ppm region of the spectrum. The data further shows that the resonances of the quaternary acetylene carbon appears after higher temperature cures in the 150-135 ppm region, and the resonances of the protonated terminal acetylene carbon move to the 125-115 ppm region. These changes correspond precisely to those predicted from the conjugated polyene structure in either the linear conformation or the trisubstituted benzene structure.

SECTION III

Fourier transform infrared spectroscopy (FTIR) offers the advantages of speed and increased signal-to-noise ratio over dispersion infrared. A dedicated computer offers the additional advantages of digitization and signal averaging making this technique a powerful tool for the characterization of polymer systems such as ATS resin. As with ^{13}C NMR, however, several difficulties posed by the system must be surmounted in order to achieve a complete description of the thermal curing mechanism.

Digitized FTIR spectra were obtained at 2 cm^{-1} resolution on Digilab FTS-14 and FTS-20E spectrometers. The FTIR spectrum of ATS monomer is shown in figure 10. The spectrum is quite crowded with absorbance bands resulting from the many strongly absorbing functional groups of the ATS monomer. The intense band located at approximately 3300 cm^{-1} results from the C-H stretching of the ethynyl groups. The $\text{C}\equiv\text{C}$ stretching band of the same ethynyl group appears only weakly at 2109 cm^{-1} . Another band that results from this terminal unsaturation is located at 942 cm^{-1} . Several overlapping bands occurring near 3050 cm^{-1} are due to the C-H stretching of the phenyl rings in the ATS chain. Phenyl ring C-H deformations give rise to bands in the 750 to 600 cm^{-1} region. Bands in the 1600 to 1400 cm^{-1} region are due to the C=C stretching and vibration modes of the phenyl rings. The doublet at about 1300 cm^{-1} and the intense band at 1150 cm^{-1} are due to

S=O stretching, while C-S stretching results in the band at 1100 cm^{-1} . The band at 1250 cm^{-1} is characteristic of aryl ether stretching of the C-O group. A complete listing of FTIR bands and their assignments is made in table 5.

The sulfone, aryl ether, and aromatic functional groups are strongly absorbing and in fact, dominate the fingerprint region of the FTIR spectra of ATS resin. This unfortunately makes difficult the detection and quantitative analysis of small changes in absorbances that would be expected upon network formation as the ATS resin cured. The structures that have been proposed to be formed upon thermal cure may absorb only weakly, if at all, and furthermore, are likely to absorb mainly in regions of the spectrum where other absorbances already exist. Several techniques developed in this laboratory have been used to confront these inherent problems. Spectral processing software has provided means for techniques such as least-square analysis, spectral subtraction, overlapping peak deconvolution, etc. Another technique, factor analysis was also applied to this system.

In this laboratory, the mathematical procedure of factor analysis has been successfully applied to series of mixture FTIR spectra for the purpose of statistically distinguishing the various components comprising the mixture. It was anticipated that this technique could also be applied to a series of spectra representing ATS resin at various stages of thermal cure. The

results of this method should distinguish a decreasing component (corresponding to the ATS monomer) and the number (if not the calculated spectra) of products that are formed upon thermal cure.

Two series of spectra were then generated. The first followed the cure of ATS resin at 150 C and the second at 180 C. The spectra were obtained at 2 cm^{-1} resolution on a Digilab FTS-14 spectrometer. The sample was prepared as a thin film of melted monomer between two KBr plates. A heating cell with proportionating control was used to allow for monitored temperature control of the sample in the instrument. Spectra were obtained at various times as the thermal polymerization proceeded for approximately 12 hours.

Twenty spectra were chosen as representative of the changes occurring over the 12 hour cure for each experiment. Each spectrum was baseline corrected and normalized with respect to the area of the deconvoluted band at 1104 cm^{-1} . This band is due to the C-S stretching mode and is known to remain constant throughout the polymerization reaction. The procedure of factor analysis was then applied to the series of spectra over the region from 1650 to 600 cm^{-1} .

The basic function of factor analysis as it has been applied to FTIR is the determination of the number of independent components present in a varying series of mixture spectra. A

data matrix is established containing raw data from the mixture spectra. The rank of this matrix corresponds to the number of components present and is given from factor analysis by the number of nonzero eigenvalues. However, because of the presence of random noise and other errors, nonzero eigenvalues arise that do not represent real components, and it becomes necessary to distinguish between significant and 'noise' eigenvalues. Several methods have been developed to make this distinction. One method is simply to plot the log eigenvalues versus the number of components. This method allows the distinction of the nonzero eigenvalues by virtue of their size and the point at which they fall to the level of 'noise' or 'error' values, which are all of similar magnitude. Unfortunately, this method can be rather ambiguous, as figure 11 shows for both the 150 C and 180 C cures.

Another method to distinguish nonzero eigenvalues is to calculate the variance associated with each eigenvector. Theoretically, the variance is a measure of the importance of an eigenvector and can therefore be used to distinguish between primary and secondary eigenvectors. In figure 12, the variance is plotted against the number of components and indicates that for both series, only secondary eigenvectors exist beyond two components.

The plot of cumulative percent variance versus number of components in figure 13, indicates that for the 150 C cure, 2 components account for virtually 100 % of the mixture spectra; while for the 180 C cure a possible third component is indicated.

Figure 14 consists of plots of real, imbedded, and extracted errors versus the number of components. Real error represents the difference between pure data, which is free from experimental error, and raw experimental data, which does contain this error. Imbedded error is the difference between the data regenerated by factor analysis, and pure data. Extracted error represents the difference between the factor analysis generated data and raw data, and is therefore the amount of error removed by factor analysis. The figure indicates that for the cure at 150 C, all errors are considerably reduced for two components, while for the 180 C cure, only with three components is the residual error reduced to very nearly zero.

The final method used in this analysis to distinguish nonzero eigenvalues is a plot of the indicator function versus the number of components. This is an empirical function which is a function of real error and often, with greater sensitivity than the real error, exhibits a minimum when the correct number of components are employed. This function is shown in figure 15 and indicates that for the 150 C cured series of spectra, 2 components are present. At 180 C this function indicates that three components comprise the mixtures.

By applying the ratio method of separation, the infrared bands that are characteristic of each contributing structure can be isolated into pure component spectra. In order to make comparisons between the two polymerization experiments, it was assumed that two components satisfactorily comprised both mixture series. Figures 16 and 17 show respectively for each the 150 C and 180 C cures the abstract spectra and the region used for ratioing and calculating the pure component spectra. Figure 18 graphically represents a plot of eigenvector components, where the shaded regions represent the meaningless event where absorbances are less than zero. The intersections of the curve and the boundary indicate the points defining the pure component spectra for each set of mixture spectra. The calculated pure spectra for the 150 C cure is shown in figure 19, while for the 180 C cure, the spectra are shown in figure 20. In each case, one of the pure component spectra clearly corresponds to ATS monomer spectrum. In fact, close examination indicates that they are almost indistinguishable. The remaining pure component spectra must then represent the product component of the polymerized resin. Although differences from the monomer spectrum are clear, there appears to be very little difference between the two product spectra. When the difference spectrum is calculated, as shown in figure 21 (150 C cure minus 180 C cure), the peak at 942 cm^{-1} is obviously not subtracted out completely. Since this peak is due to $\equiv\text{C-H}$ deformations, exactly as would be expected, the analysis indicates that the 150 C cured ATS has not

have achieved the degree of cure of the 180 C cured ATS.

Degree of cure as a function of time was determined by analysis of both the band at 3300 cm^{-1} which is due to $\equiv\text{C-H}$ stretching and the band at 942 cm^{-1} which is again due to $\equiv\text{C-H}$ deformation. A least-squares curve-fitting technique was employed to quantitatively establish the degree of cure according to the band at 3300 cm^{-1} . This reaction parameter is illustrated in figure 22 in the form of percent decrease in peak area for both the 150 C and 180 C cures. Not only did the sample cured at 180 C initially polymerize at a faster rate, but after 12 hours, it had reacted substantially more of its acetylene groups. Because of the broadening and overlapping of peaks as the polymerization proceeded, least-squares curve-fitting could not accurately be applied to the analysis of the 942 cm^{-1} band. Instead, a routine was utilized that enabled the fit of Lorentzian-shaped curves to the spectral region. The region from 995 to 754 cm^{-1} was fit with five Lorentzian curves to obtain more accurately the area of the 942 cm^{-1} band. The area of the deconvoluted band as a percent of the monomer band was plotted versus cure time for both experiments (figure 23). The curves for the 942 cm^{-1} band and the 3300 cm^{-1} band are very similar.

Cure studies also focussed on the effect of high-temperature postcures of ATS resin. Bulk ATS monomer was initially cured using an oil bath maintained at precisely 150 C. The material was subjected to cure times of 60, 180, and 720 minutes. From

these three base samples, postcures were conducted at a temperature of 300 C for all samples. From each base sample, material was postcured for 10, 20, and 30 minutes. Two sets of spectra were recorded for each postcured sample. One set of KBr pellets were made thin and with low concentration of sample in order to keep absorbances within the linear portion of the Beer-Lambert relation. The second set of KBr pellets were made thick and more concentrated in order to gain resolution of any weak bands that may be useful in the characterization of cure mechanisms. The FTIR spectra were obtained at 2 cm^{-1} on a Digilab FTS-20E spectrometer.

Normalization of the spectra obtained from the less concentrated KBr pellets was accomplished, after baseline correction, by the deconvolution of the 1104 cm^{-1} band. Again, the area of this band, which is due to the C-S stretching mode, is known to remain constant throughout the polymerization reaction. Degree-of-cure (DOC) values were then obtained by measurement of the area of the band at 3300 cm^{-1} for each sample. This band is due to $\equiv\text{C-H}$ stretching, and is the best quantitative measure of terminal acetylene loss because no interference from adjacent peaks occurs. Figure 24 incorporates both the pre- and postcure DOC values, measured from this peak, for the various samples. The base samples, cured at 150 C, exhibited rapid initial cure, then a slower increase toward 100% cure. When the base samples were postcured at 300 C, the DOC neared complete

cure within the first 10 minutes followed by a more gradual approach toward 100%.

Several regions of the infrared spectra obtained from these samples exhibit slight, but possibly significant changes. A very weak band that occurs at 2334 cm^{-1} is noted as sharply increasing in various of the postcured samples. This band has been proposed to be due to "chain acetylenes". In the first sample to be postcured (base sample cured 1 hr at 150 C), this peak appears to increase with postcures of 10 and 20 minutes at 300 C (figure 25). Upon further cure, the band decreases somewhat and remains constant. For the base material that was cured 3 hrs at 150 C (figure 26), no increase occurs until the sample was cured for 30 minutes at 300 C. The final base sample showed erratic changes in this peak (figure 27). Although changes are evident, no systematic behavior is yet observed. Assignment of this band to chain acetylenes appears somewhat questionable, in that disubstituted acetylenes only rarely are known to absorb as high as 2300 cm^{-1} , and then, it appears, due to the high electronegativity of the substituent groups. The change, however, is apparent and further study of the peak's behavior with cure and possible assignment is merited.

A band at 948 cm^{-1} appears to result from the 300 C postcure. This band was not detected in any of the base samples that were cured at 150 C. Figures 28 to 30 show that a slight shoulder or asymmetry of the 942 cm^{-1} band increases with

postcure time for all three base samples. This new peak finally predominates after 30 minute postcures for two of the samples while the 942 cm^{-1} band decreases with the DOC of the material. The band appears to be broad, but is superimposed on both the 942 cm^{-1} and the 965 cm^{-1} bands, making both detection and quantitative characterization difficult. Assignment is not certain, although various unsaturated hydrogen out-of-plane deformations occur in this region. Spectral processing of this region with initial attempts at deconvolution have not yet been conclusive. This band is particularly interesting in that it appears to be unique to the high-temperature postcure. The band at 965 cm^{-1} also appears to increase slightly upon postcure, while at the 150 C cure, it seems not to significantly change with time. This peak can possibly be assigned to the hydrogen out-of-plane deformation of a trans-disubstituted ethylene group.

LIST OF TABLES

TABLE	PAGE
1. Calculated and observed chemical shifts for ATS monomer carbons.	30
2. Calculated chemical shifts for cyclotrimerized products.	31
3. Percent contribution breakdown for ^{13}C NMR spectra of ATS resin.	32
4. Percent of 150-110 ppm band due to protonated and quaternary carbons for ^{13}C NMR spectra of cured ATS resin. Also listed are T_2 's for protonated and quaternary carbons.	33
5. FTIR bands and assignments for ATS monomer.	34

LIST OF ILLUSTRATIONS

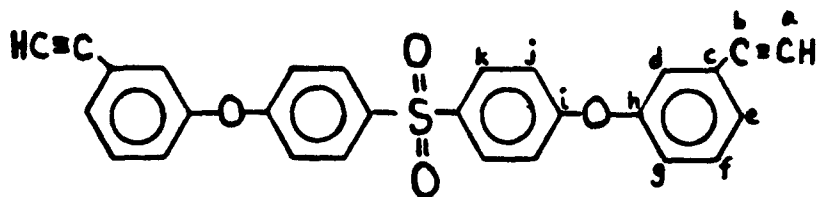
FIGURE	PAGE
1. ^{13}C NMR spectra of ATS monomer spinning in a Delrin rotor at 3.8 KHz and in a Kel-F rotor at 2.3 KEz.	35
2. a) ^{13}C NMR cross-polarization spectrum of ATS monomer with corresponding assignments and b) ^{13}C NMR protonated carbon suppression spectrum of ATS monomer with assignments.	36
3. ^{13}C NMR spectra of ATS cured for various times at 120 C.	37
4. a) ^{13}C NMR spectrum of ATS cured 12 hours at 120 C, b)ATS cured 1 hour at 120C, and c)difference spectrum of a - b.	38
5. ^{13}C NMR spectra of ATS monomer with artificial line broadening and ATS cured at various times and temperatures.	39
6. ^{13}C NMR spectra of ATS cured 10 minutes at 300 C for various T_{DD} values in the dipolar dephasing pulse sequence.	40
7. Plot of the decay of magnetization of the aromatic band with T_{DD} (delay time). Data points are fit with a combination Gaussian-Lorentzian curve.	41
8. a) ^{13}C NMR spectrum of ATS cured 10 minutes at 300 C, b)ATS monomer with artificial line broadening, and c)difference spectrum of a - b.	42
9. a) ^{13}C NMR spectrum of ATS cured 10 minutes at 300 C, b)ATS cured 12 hours at 120 C, and c) difference spectrum of a - b.	43
10. FTIR spectra of ATS monomer.	44
11. Log eigenvalues vs. number of components calculated for mixture spectra of ATS cure at a)150 C and b)180 C.	45
12. Variance vs. number of components calculated for mixture spectra of ATS cure at a)150 C and b)180 C.	46
13. Cumulative percent variance vs. number of components calculated for mixture spectra of ATS cure at a)150 C and b)180 C.	47

FIGURE	PAGE
14. Real, embedded and extracted errors vs. number of components calculated for mixture spectra of ATS cure at a)150 C and b)180 C.	48
15. Indicator function vs. number of components calculated for mixture spectra of ATS cure at a)150 C and b)180 C.	49
16. Regions of abstract spectra used to calculate pure component spectra for ATS cure at 150 C. Dotted lines indicate ratio region.	50
17. Regions of abstract spectra used to calculate pure component spectra for ATS cure at 180 C. Dotted lines indicate ratio region.	51
18. Plot of relative positions of mixture spectra and pure component spectra for ATS cure at a)150 C and b)180 C.	52
19. Calculated pure spectra from mixture spectra of ATS cure at 150 C.	53
20. Calculated pure spectra from mixture spectra of ATS cure at 180 C.	54
21. Difference spectra between pure components corresponding to products of ATS cure at 180 C and 150 C.	55
22. Percentage of acetylene loss as measured from band at 3300 cm^{-1} for ATS cure at 150 C and 180 C.	56
23. Percentage of acetylene loss as measured from band at 942 cm^{-1} for ATS cure at 150 C and 180 C.	57
24. Degree of cure as measured from 3300 cm^{-1} band versus time of cure at 150 C and postcures at 300 C.	58
25. FTIR spectra of ATS cured 1 hr at 150 C and postcured for various times at 300 C.	59
26. FTIR spectra of ATS cured 3 hrs at 150 C and postcured for various times at 300 C.	60
27. FTIR spectra of ATS cured 12 hrs at 150 C and postcured for various times at 300 C.	61

FIGURE	PAGE
28. FTIR spectra of ATS cured 1 hr at 150 C and postcured for various times at 300 C.	62
29. FTIR spectra of ATS cured 3 hrs at 150 C and postcured for various times at 300 C.	63
30. FTIR spectra of ATS cured 12 hrs at 150 C and postcured for various times at 300 C.	64

TABLE 1

Calculated and observed chemical shifts for ATS monomer carbons.

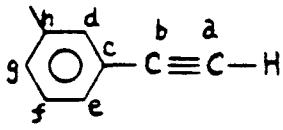
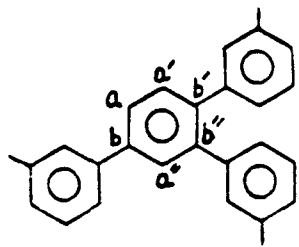
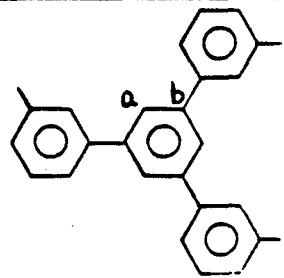


<u>Carbon</u>	<u>calc. δ (ppm)</u>	<u>observed δ (ppm)</u>
a		82.2
b		82.5
c	124.0	125.4
d	122.9	121.4
e	127.2	129.9
f	130.5	132.8
g	118.9	116.5
h	158.1	152.9
i	164.4	162.4
j	114.9	126.5
		125.0
k	128.8	131.2
		130.8
l	133.3	135.6

TABLE 2

Calculated chemical shifts for cyclotrimerization products

ACETYLENE CARBONS

<u>Monomer</u>	<u>1,2,4-trisubstitution</u>	<u>1,3,5-trisubstitution</u>
		
<u>carbon</u> <u>obsvd δ</u>	<u>carbon</u> <u>calc δ</u>	<u>carbon</u> <u>calc δ</u>
a 82.2	a 126.6	a 125.1
b 82.5	b 140.8	b 142.4
	a' 128.2	
	b' 126.7	
	a'' 126.7	
	b'' 140.9	

PENDANT AROMATIC CARBONS

<u>Monomer</u>	<u>1,2,4- and 1,3,5-trisubstitution</u>
<u>carbon</u> <u>calc δ</u>	<u>carbon</u> <u>calc δ</u>
c 124.0	c' 143.2
d 122.9	d' 118.0
e 127.2	e' 122.3
f 130.5	f' 130.5 (same)
g 118.9	g' 117.9
h 158.1	h' 158.1 (same)

TABLE 3

Percent contribution breakdown for ^{13}C NMR spectra of
ATS resins.

<u>Cure state of ATS resin</u>	<u>^{13}C NMR band</u>	<u>% of total area</u>
Monomer	acetylene	14.4
	150-110 ppm	71.6
	aryl ether	14.0
3 hrs/150 C	acetylene	0.0
	150-110 ppm	87.3
	aryl ether	12.7
10 min/300 C	acetylene	0.0
	150-110 ppm	88.6
	aryl ether	11.4
3 hrs/150C and 10 min/300 C	acetylene	0.0
	150-110 ppm	88.5
	aryl ether	11.5

TABLE 4

Percent of 150-110 ppm band due to protonated and quaternary carbons for ^{13}C NMR spectra of cured ATS resins. Also listed are T_2 's for protonated and quaternary carbons.

<u>Cure state of ATS resin</u>	<u>Carbon type</u>	<u>% area of 150-110 ppm band</u>	<u>T_2^* (μsec)</u>
Monomer	protonated	77.3	-
	quaternary	22.7	-
3 hrs/150 C	protonated	72.3	16.4
	quaternary	27.7	276.4
10 min/300 C	protonated	73.1	15.7
	quaternary	26.9	233.6
3 hrs/150 C and 10 min/300 C	protonated	72.0	14.5
	quaternary	28.0	184.6

TABLE 5
FTIR bands and assignments of ATS monomer.

wavenumber	assignment
3266	\equiv C-H str.
3093	aromatic C-H str.
3073	aromatic C-H str.
2109	mono-substituted C \equiv C str.
1592	aromatic ring in-plane str.
1571	aromatic ring in-plane str.
1491	para-disubstituted aromatic ring in-plane str.
1479	meta-disubstituted aromatic ring in-plane str.
1425	aromatic ring in-plane vib.
1314	S=O str.
1294	S=O str.
1250	C-O str.
1224	para-disub. aromatic ring hydrogen in-plane vib.
1173	S=O str.
1152	S=O str.
1132	S=O str.
1106	C-S str.
1081	aromatic ring hydrogen in-plane vib.
1072	aromatic ring hydrogen in-plane vib.
1005	aromatic ring hydrogen in-plane vib.
1001	aromatic ring hydrogen in-plane vib.
965	hydrogen out-of-plane def. of trans-disub. ethylene
941	\equiv C-H hydrogen out-of-plane def.
906	meta-disub. aromatic ring hydrogen out-of-plane str.
892	meta-disub. aromatic ring hydrogen out-of-plane str.
840	
823	para-disub. aromatic ring hydrogen out-of-plane str.
791	meta-disub. aromatic ring hydrogen out-of-plane str.
740	
717	hydrogen out-of-plane def. of cis-disub. ethylene
698	meta-disub. aromatic ring hydrogen out-of-plane vib.
654	\equiv C-H hydrogen bending mode
625	\equiv C-H hydrogen bending mode
575	SO ₂ scissoring mode

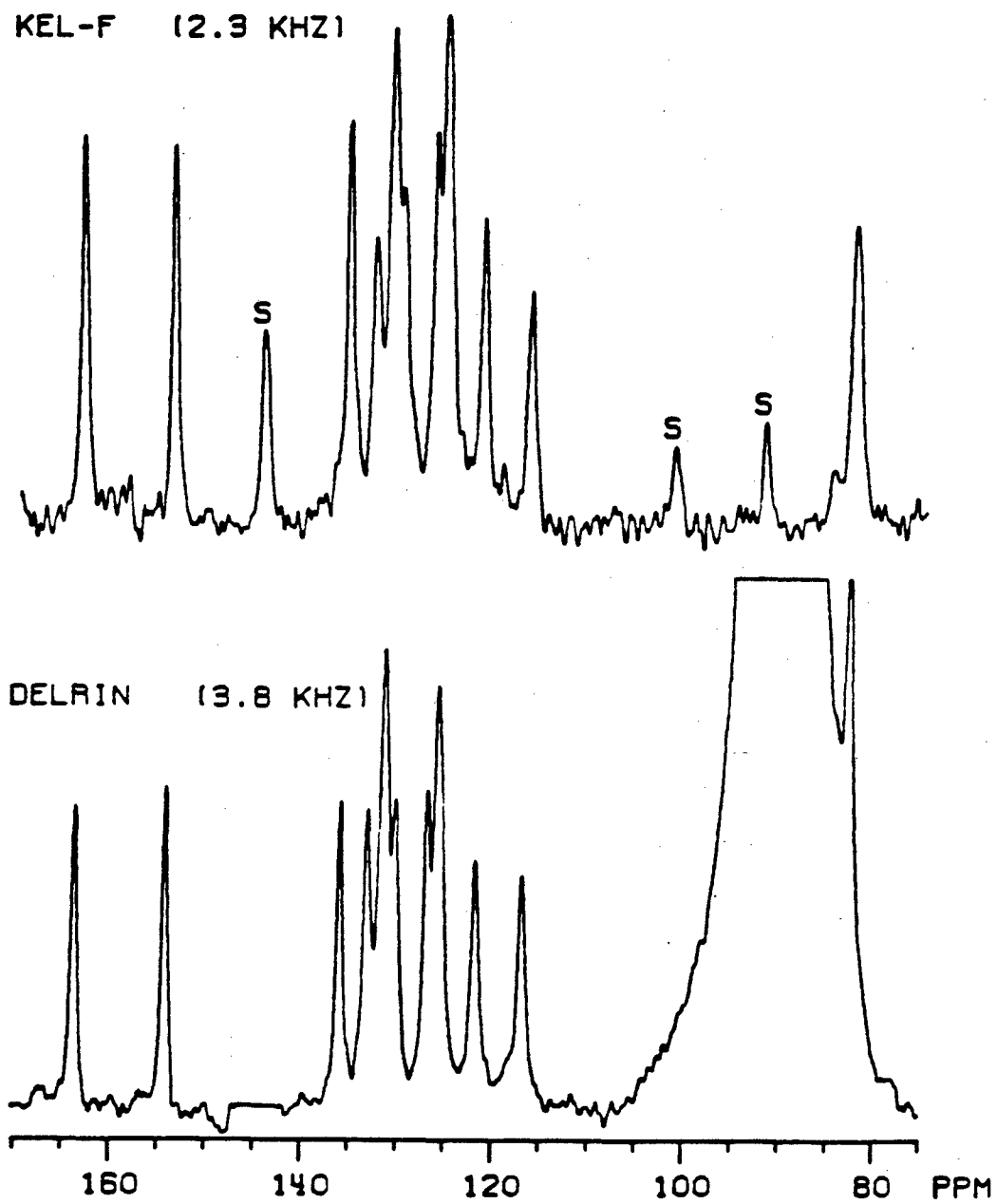


Figure 1. ^{13}C NMR spectra of ATS monomer spinning in a Delrin rotor at 3.8 KHz and in a Kel-F rotor at 2.3 KHz.

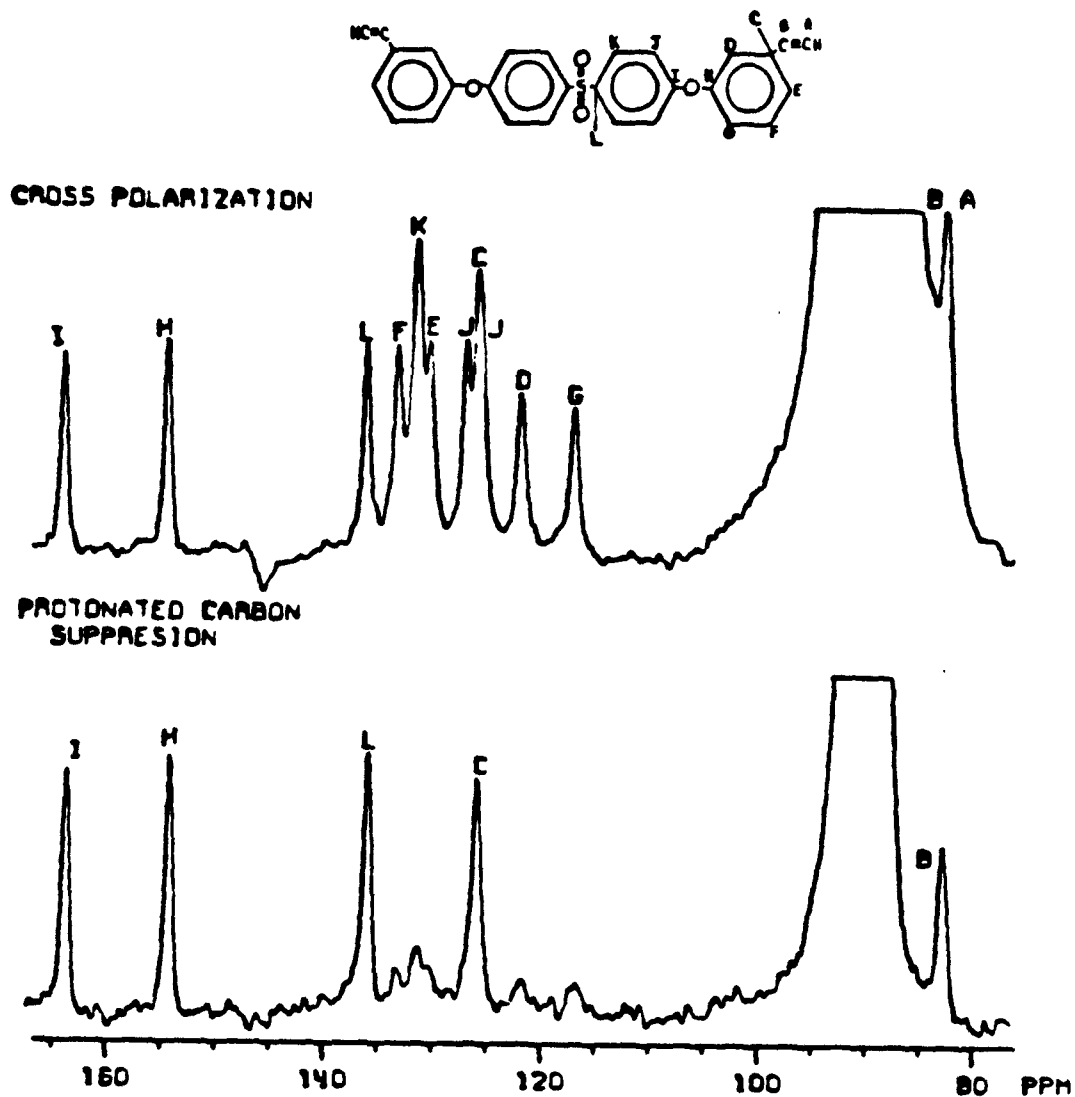


Figure 2. a) ^{13}C NMR cross-polarization spectrum of ATS monomer with corresponding assignments and b) ^{13}C NMR protonated carbon suppression spectrum of ATS monomer with assignments.

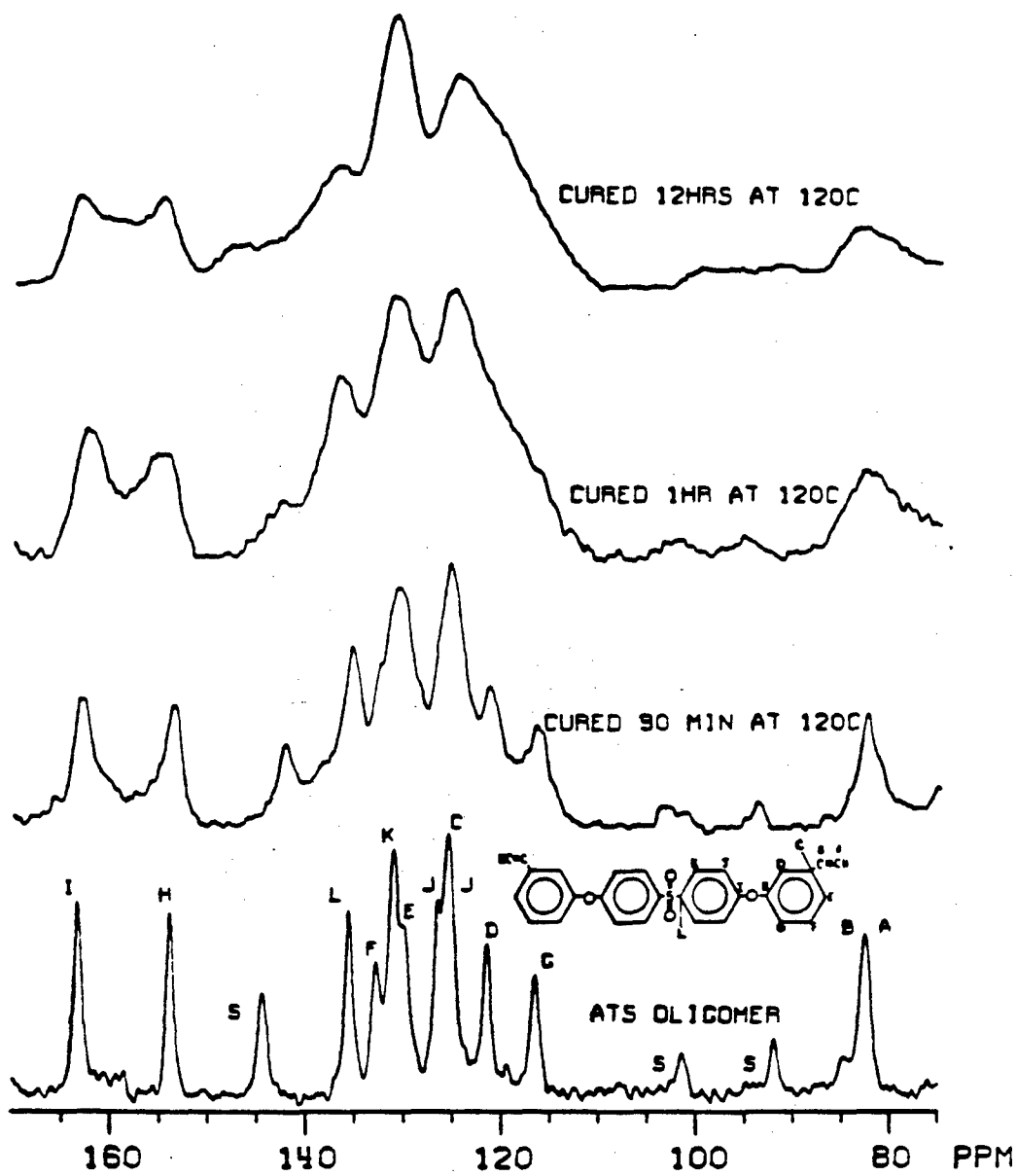


Figure 3. ^{13}C NMR spectra of ATS cured for various times at 120 C.

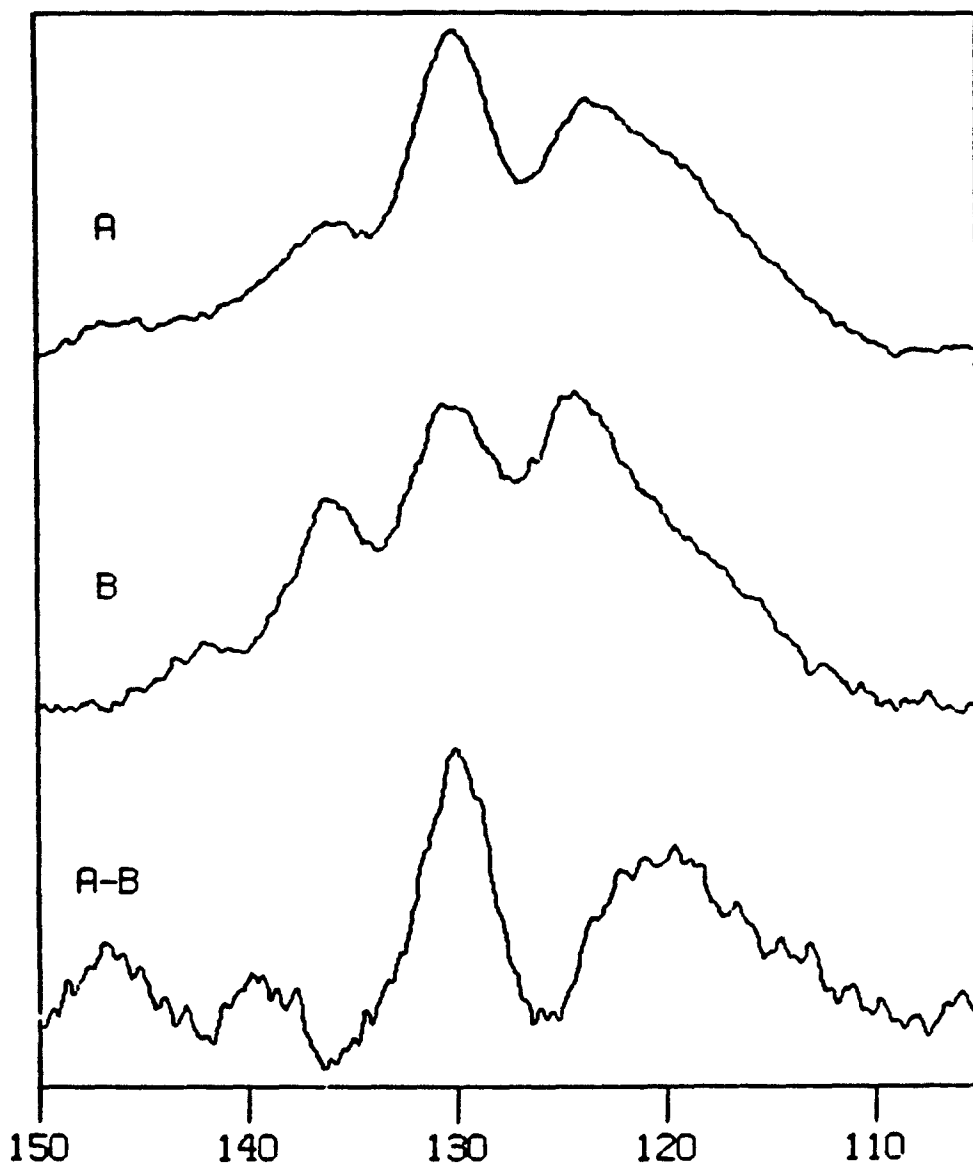


Figure 4. a) ^{13}C NMR spectrum of ATS cured 12 hours at 120 C, b) ATS cured 1 hour at 120C, and c) difference spectrum of a - b.

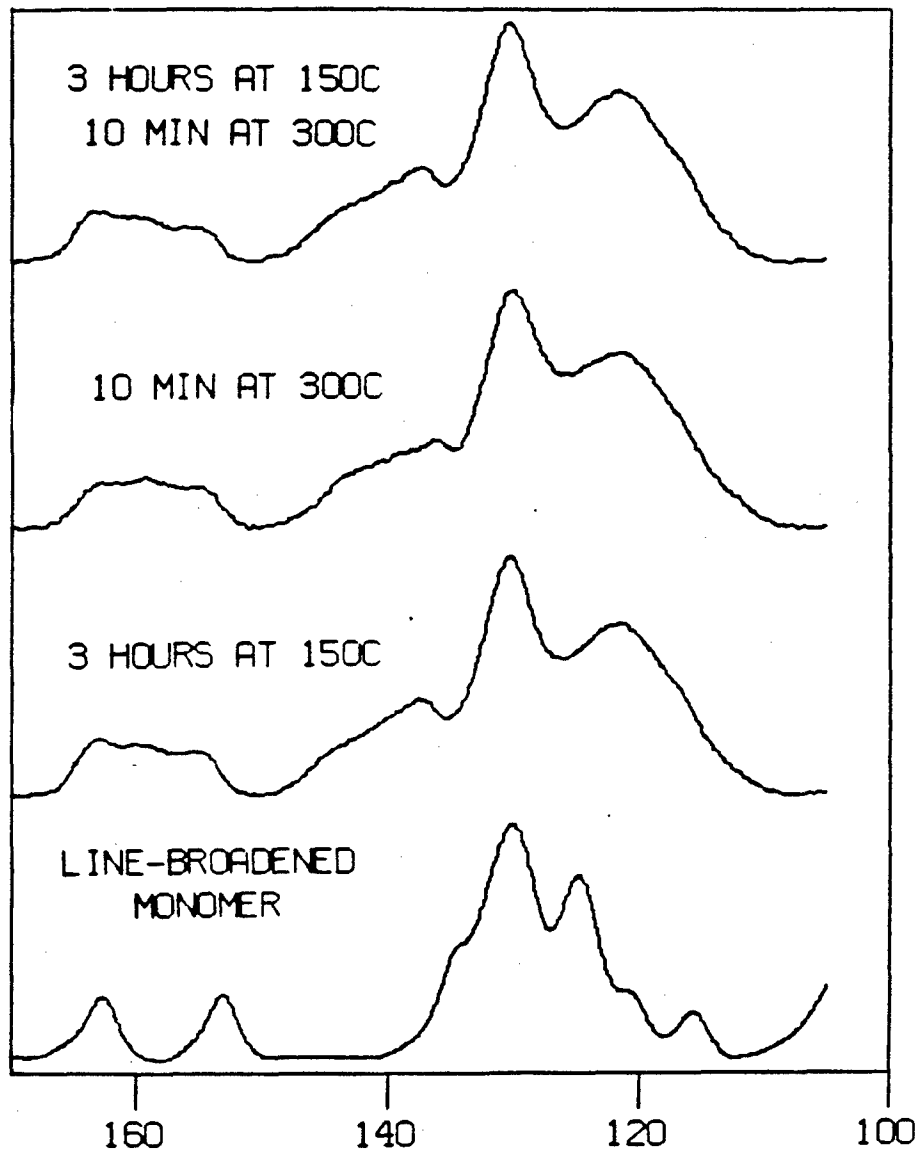


Figure 5. ^{13}C NMR spectra of ATS monomer with artificial line broadening and ATS cured at various times and temperatures.

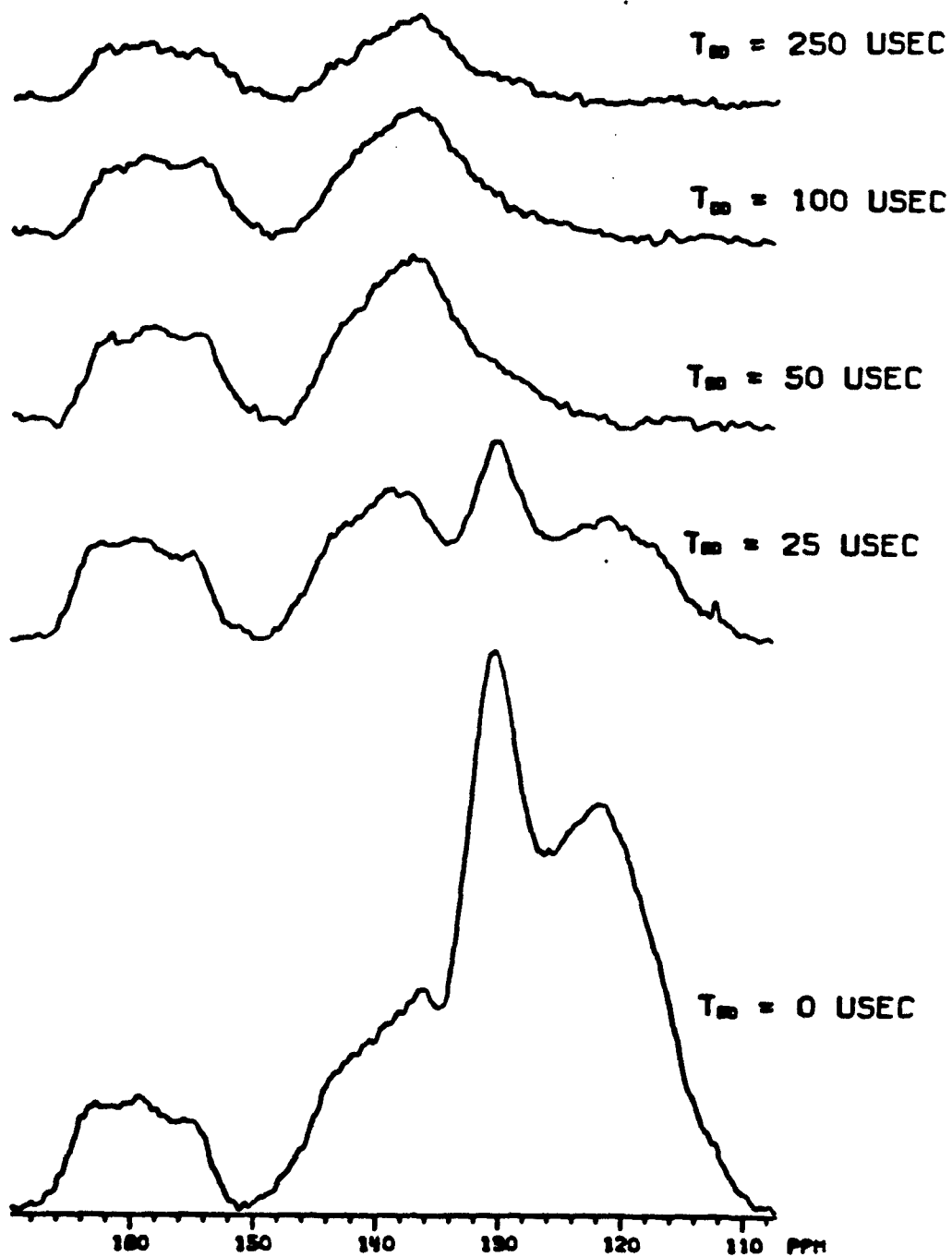


Figure 6. ^{13}C NMR spectra of ATS cured 10 minutes at 300 C for various T_{DD} values in the dipolar dephasing pulse sequence.

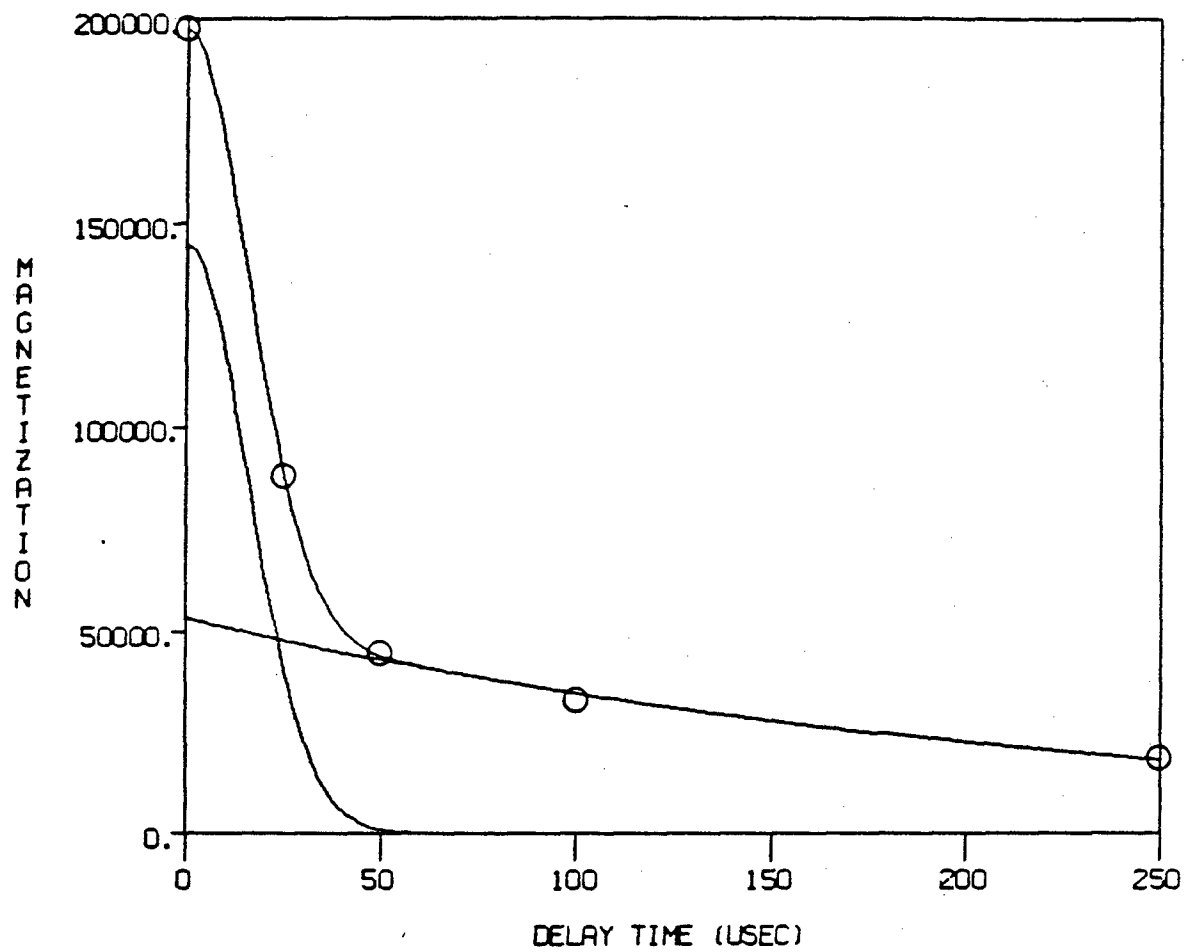


Figure 7. Plot of the decay of magnetization of the aromatic band with T_{DD} (delay time). Data points are fit with a combination Gaussian-Lorentzian curve.

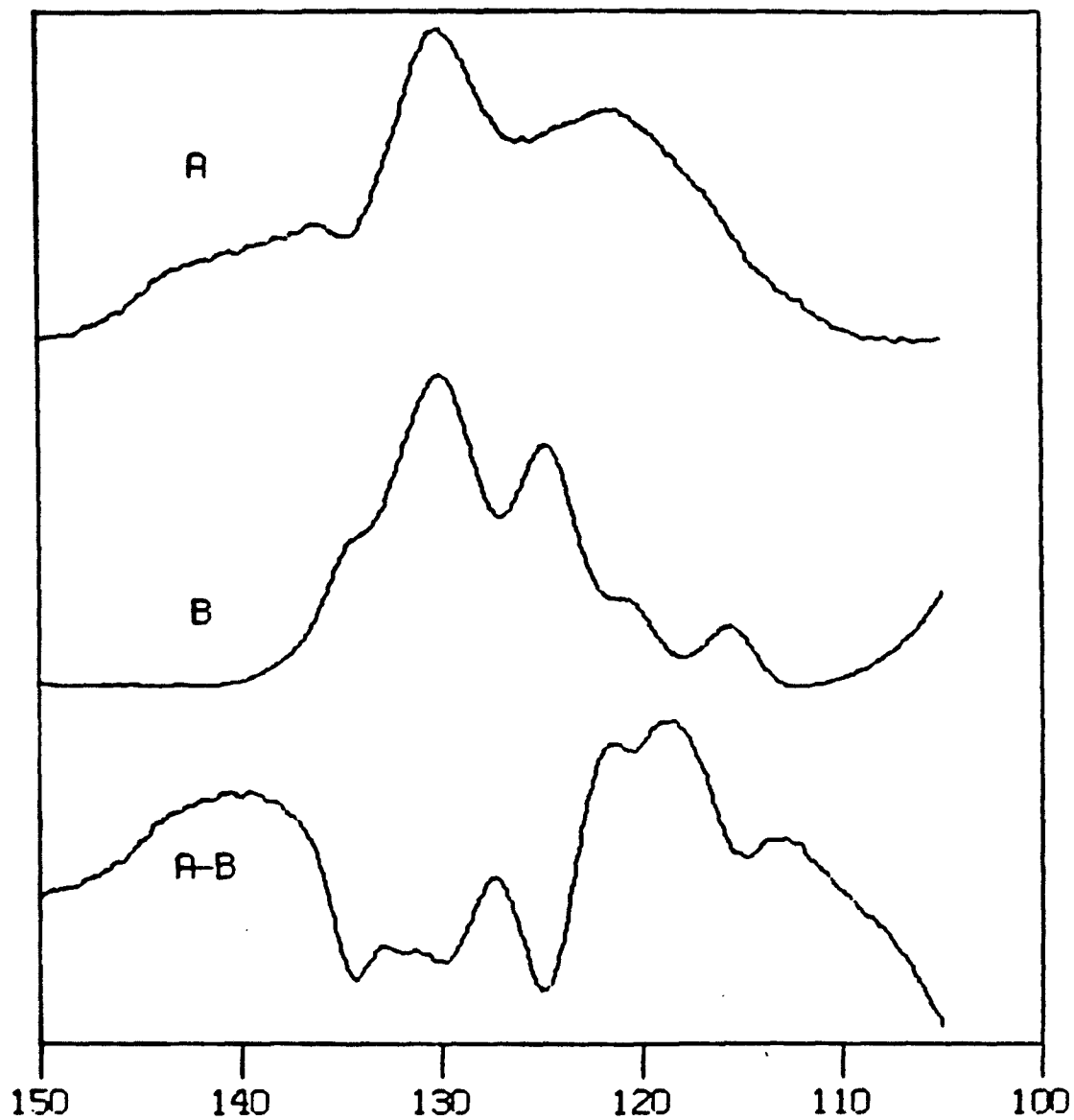


Figure 8. a) ^{13}C NMR spectrum of ATS cured 10 minutes at 300 C, b) ATS monomer with artificial line broadening, and c) difference spectrum of a - b.

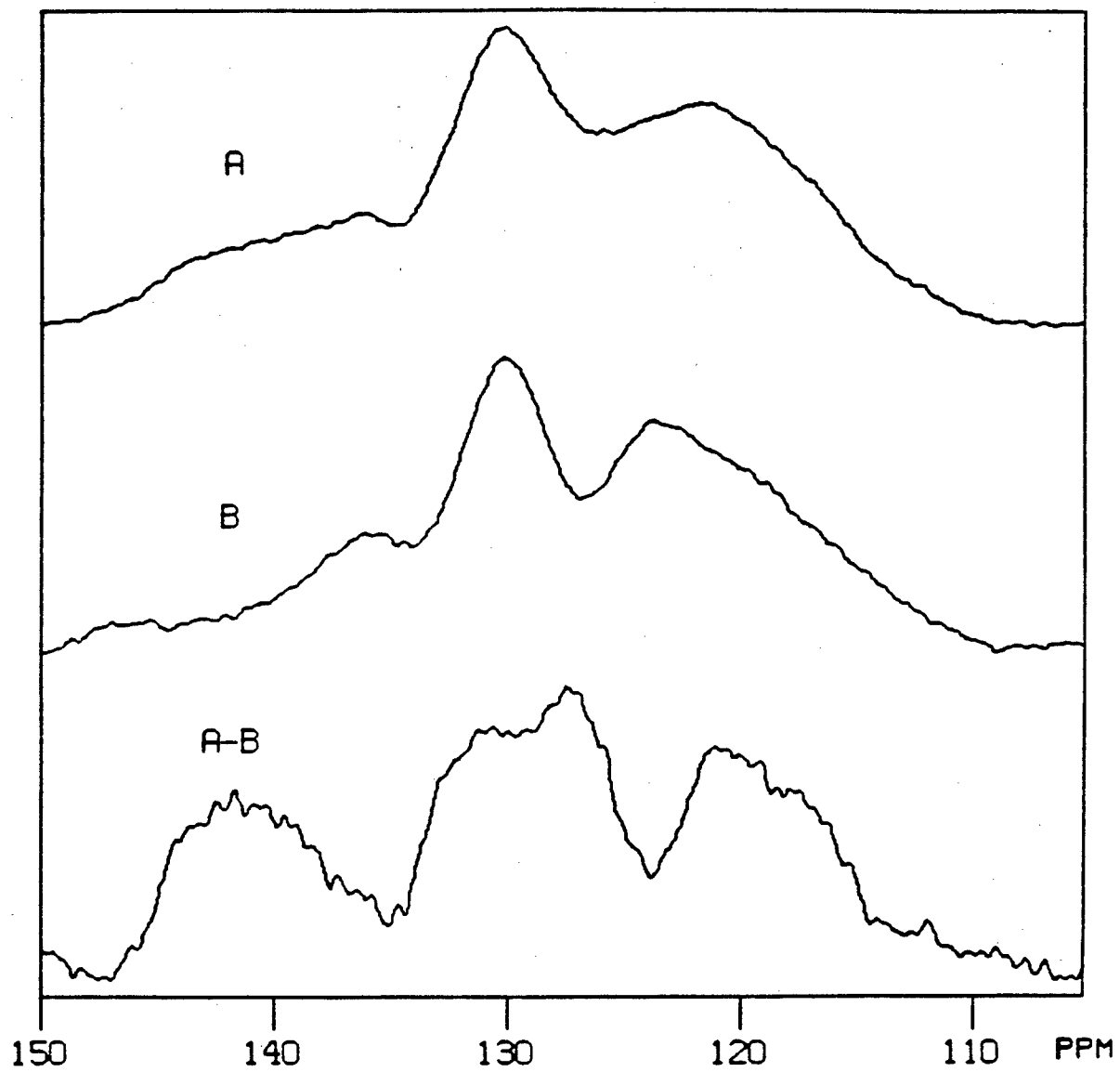


Figure 9. a) ^{13}C NMR spectrum of ATS cured 10 minutes at 300 C, b) ATS cured 12 hours at 120 C, and c) difference spectrum of a - b.

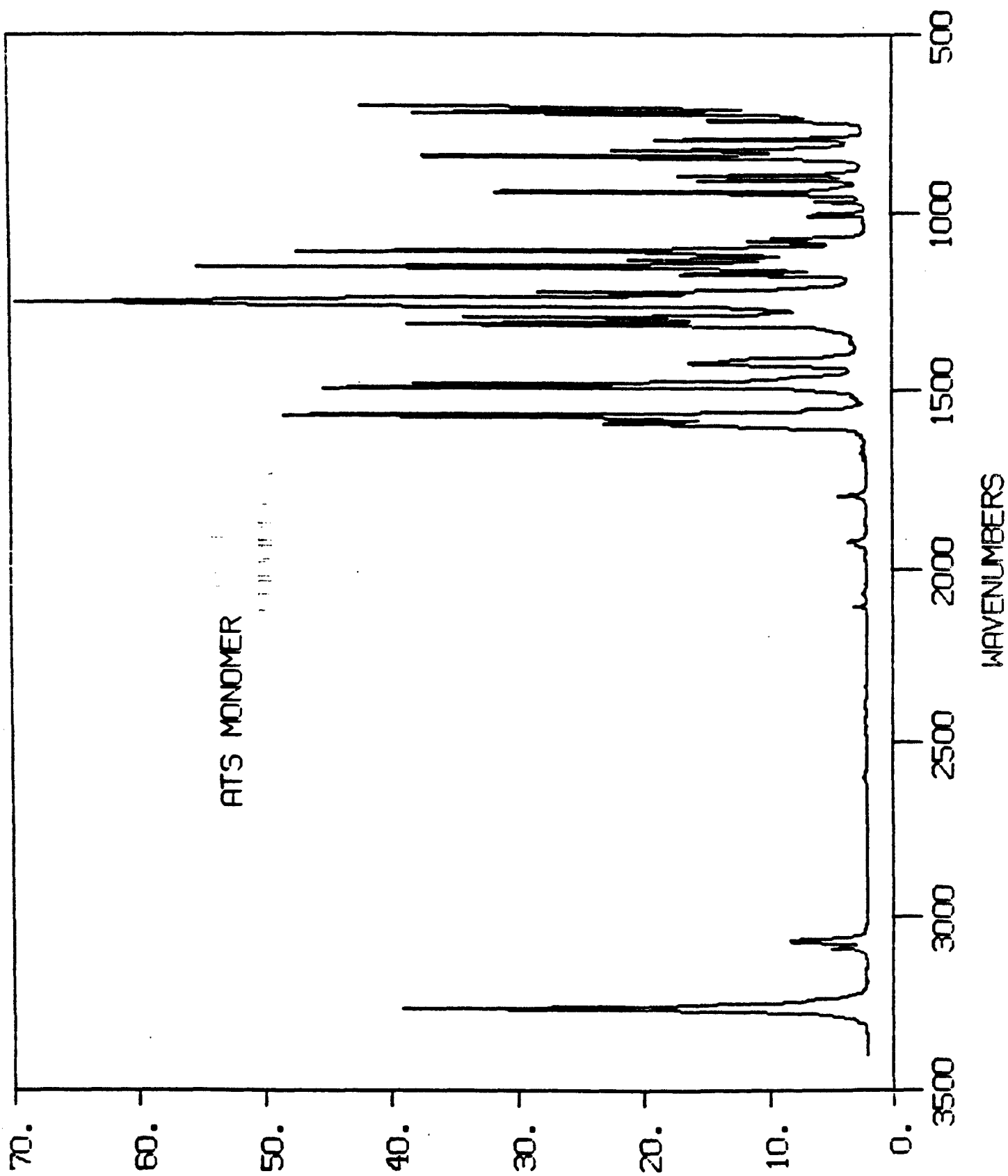


Figure 10. FTIR spectra of ATS monomer.

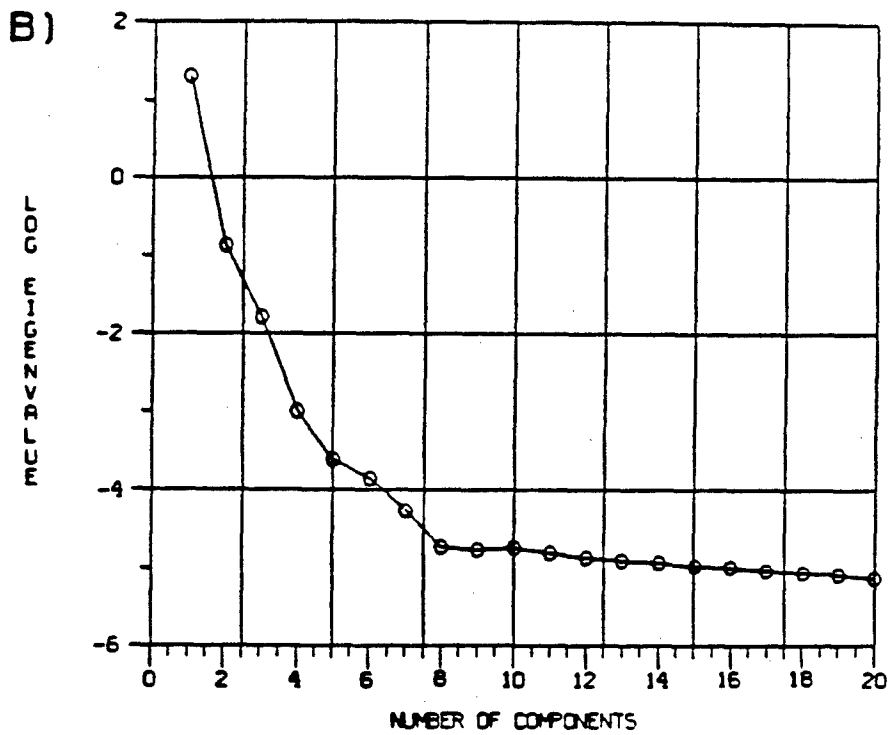
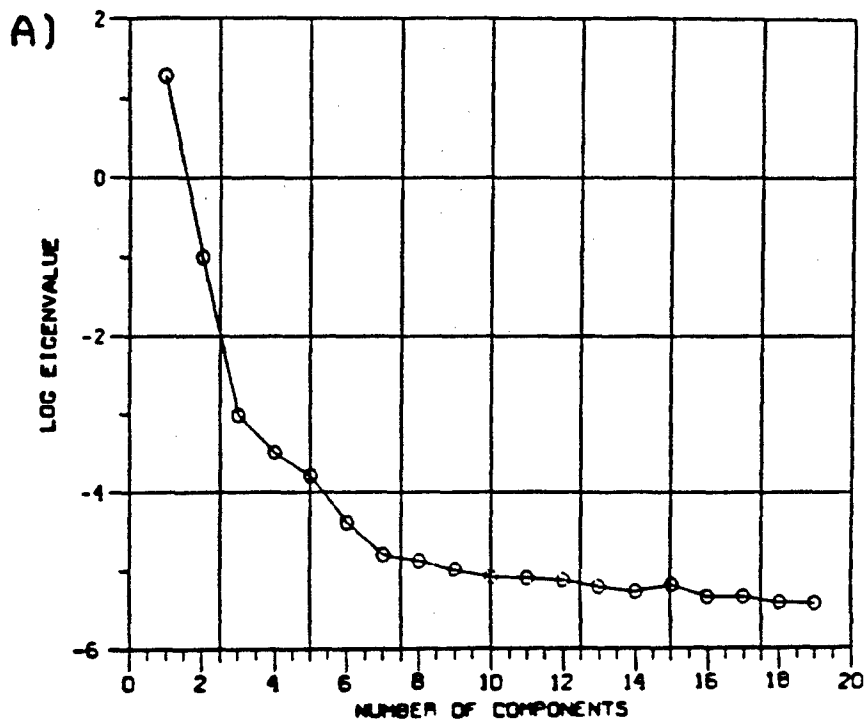


Figure 11. Log eigenvalues vs. number of components calculated for mixture spectra of ATS cure at a)150 C and b)180 C.

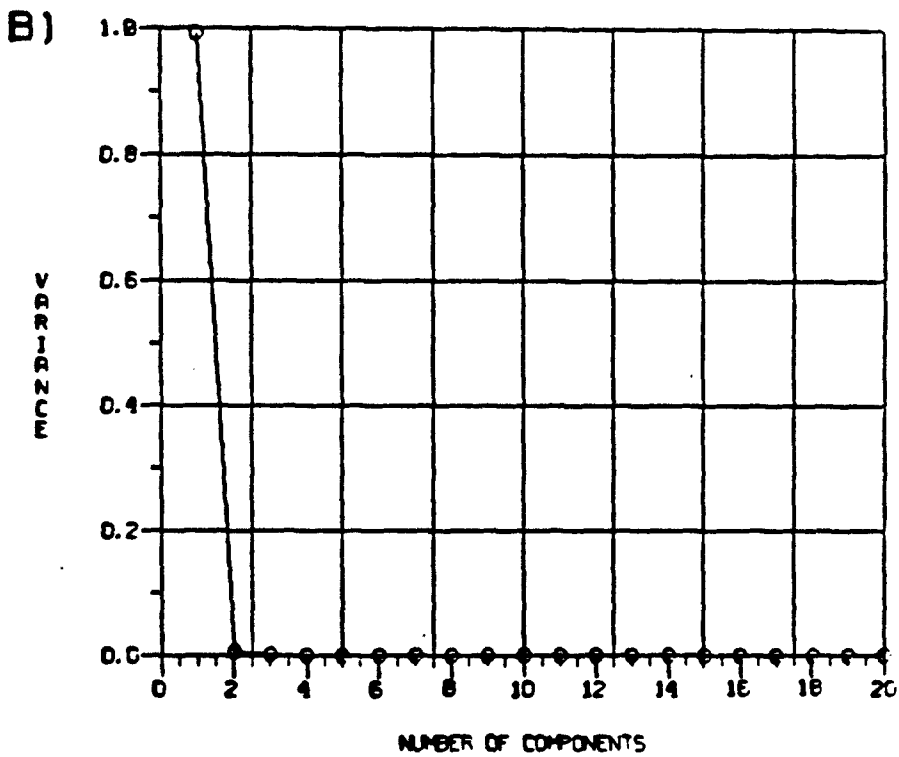
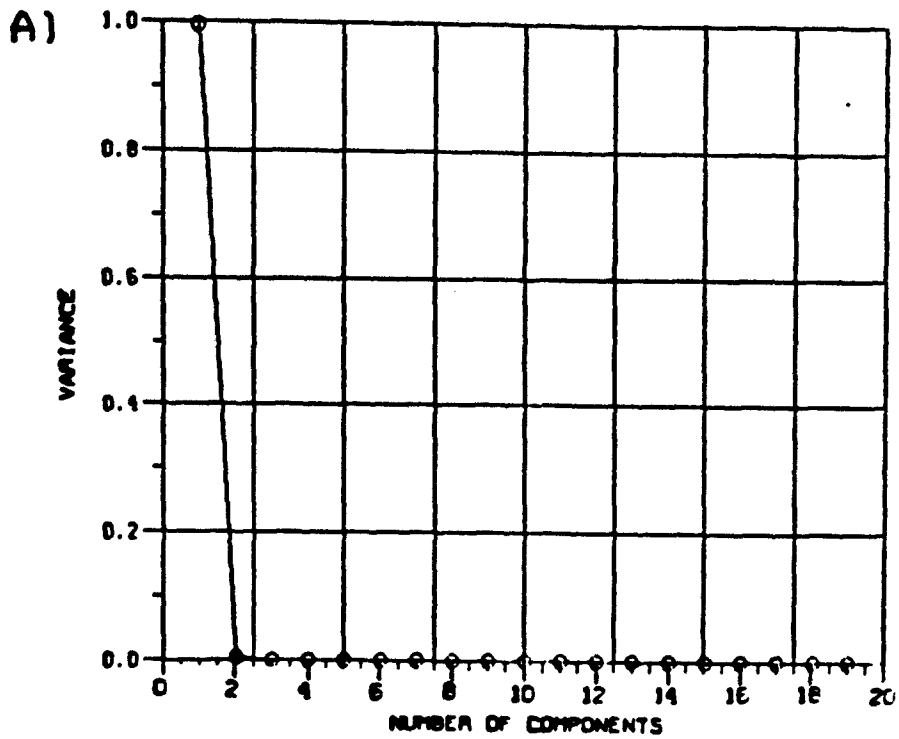
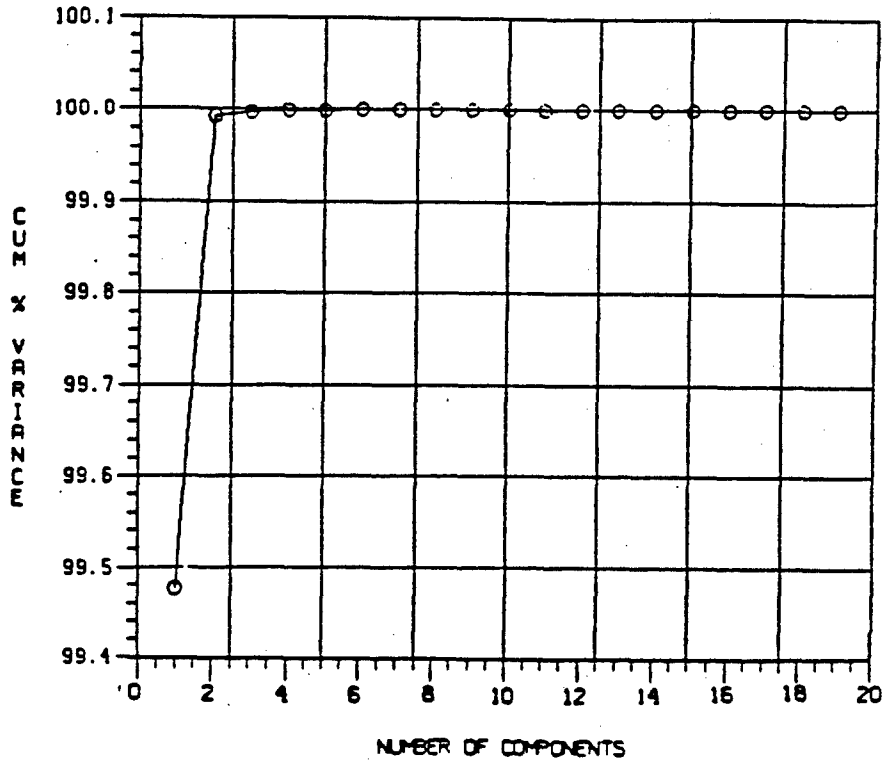


Figure 12. Variance vs. number of components calculated for mixture spectra of ATS cure at a)150 C and b)180 C.

A)



B)

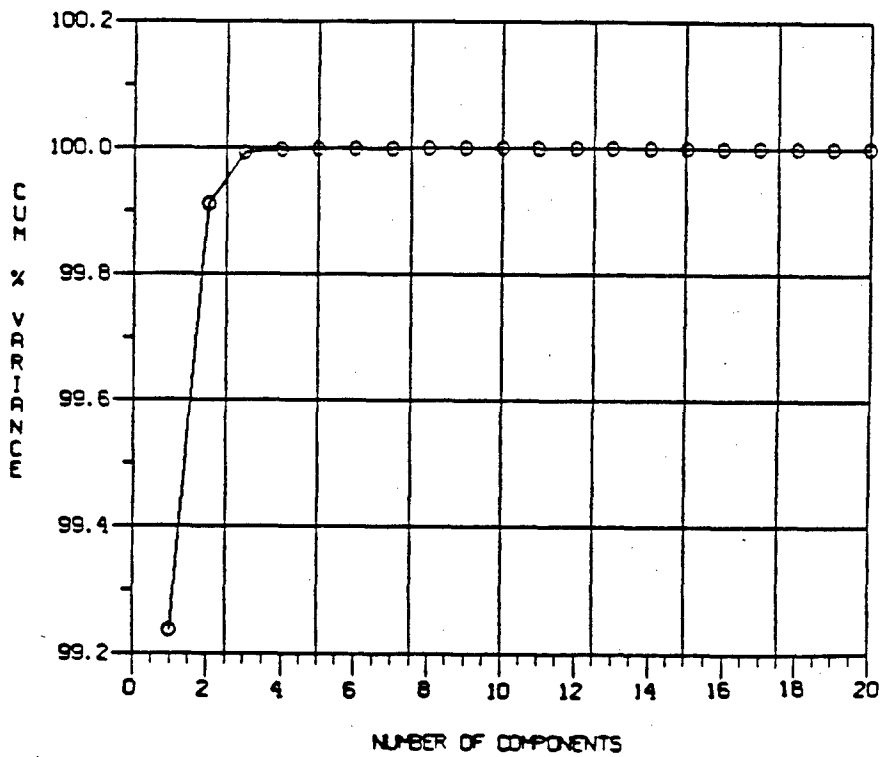


Figure 13. Cumulative percent variance vs. number of components calculated for mixture spectra of ATS cure at a)150 C and b)180 C.

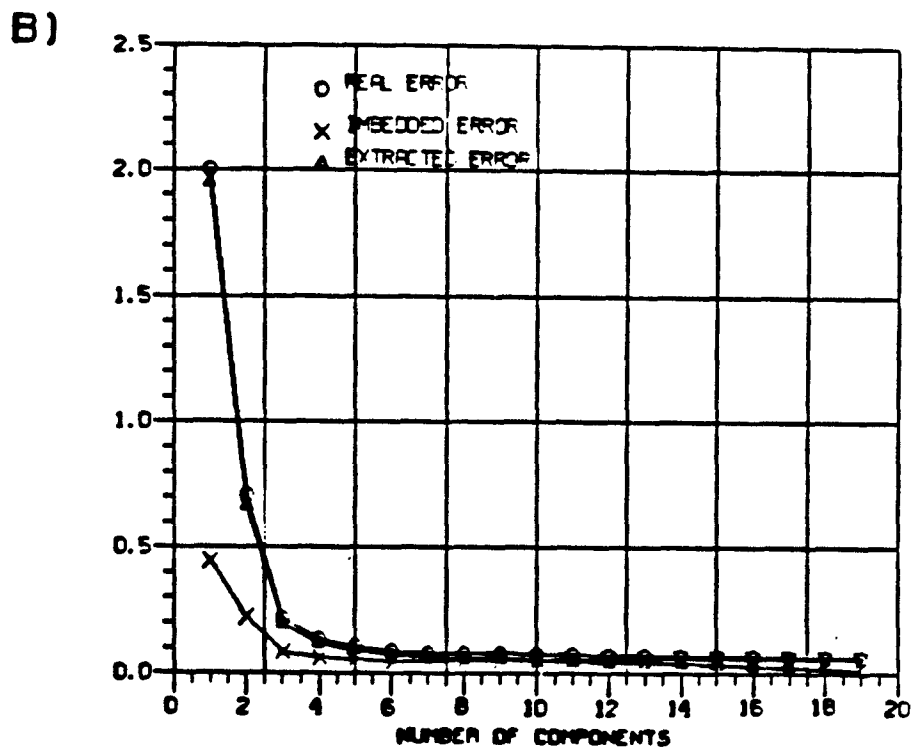
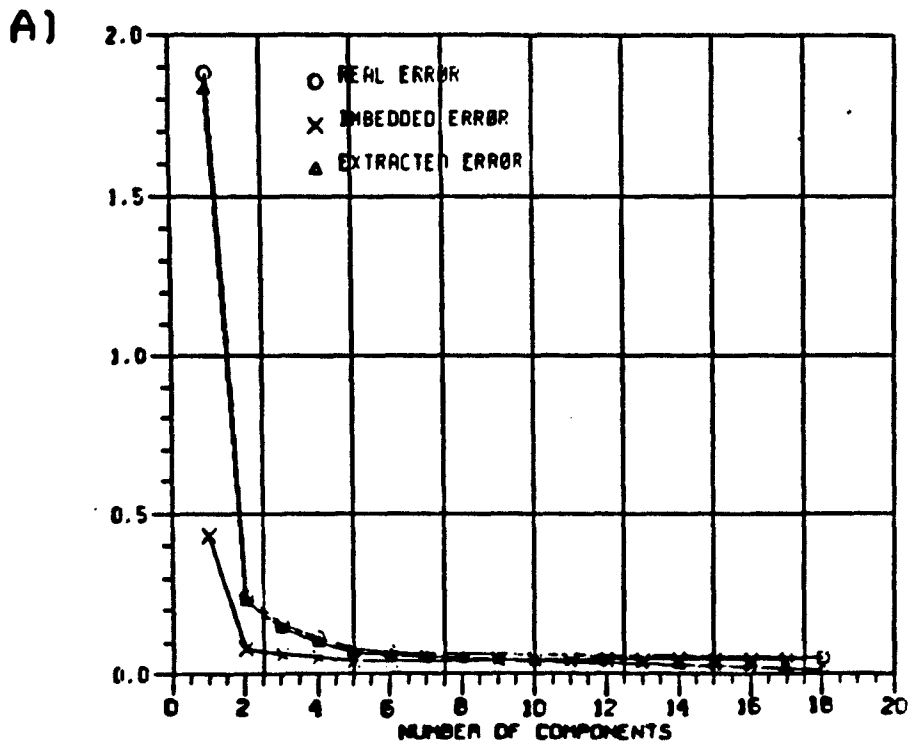


Figure 14. Real, embedded and extracted errors vs. number of components calculated for mixture spectra of ATS cure at a)150 C and b)180 C.

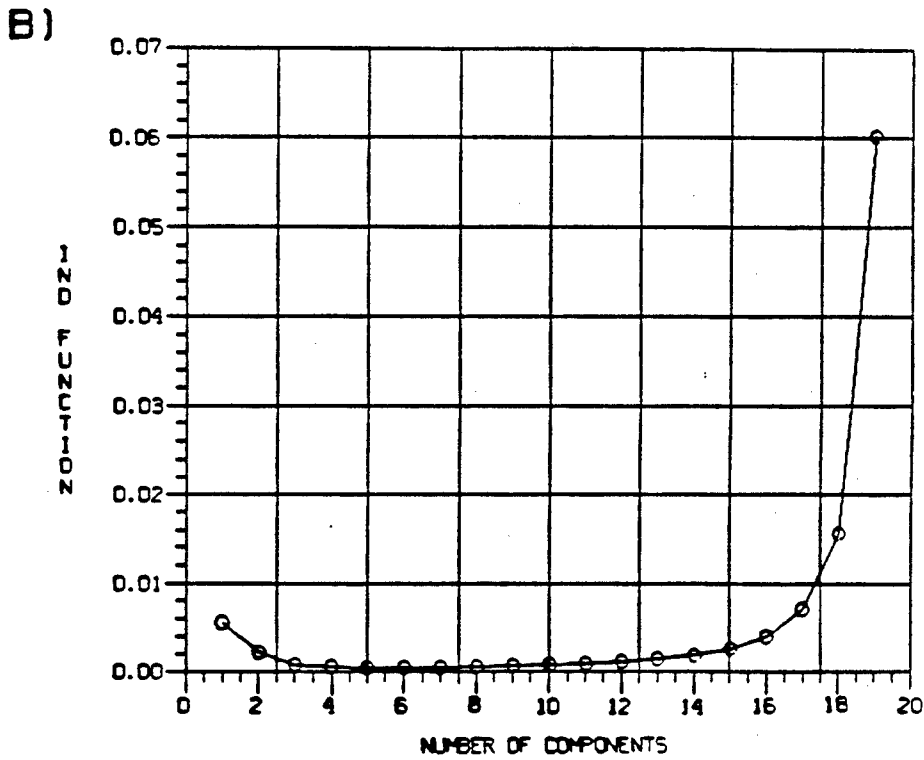
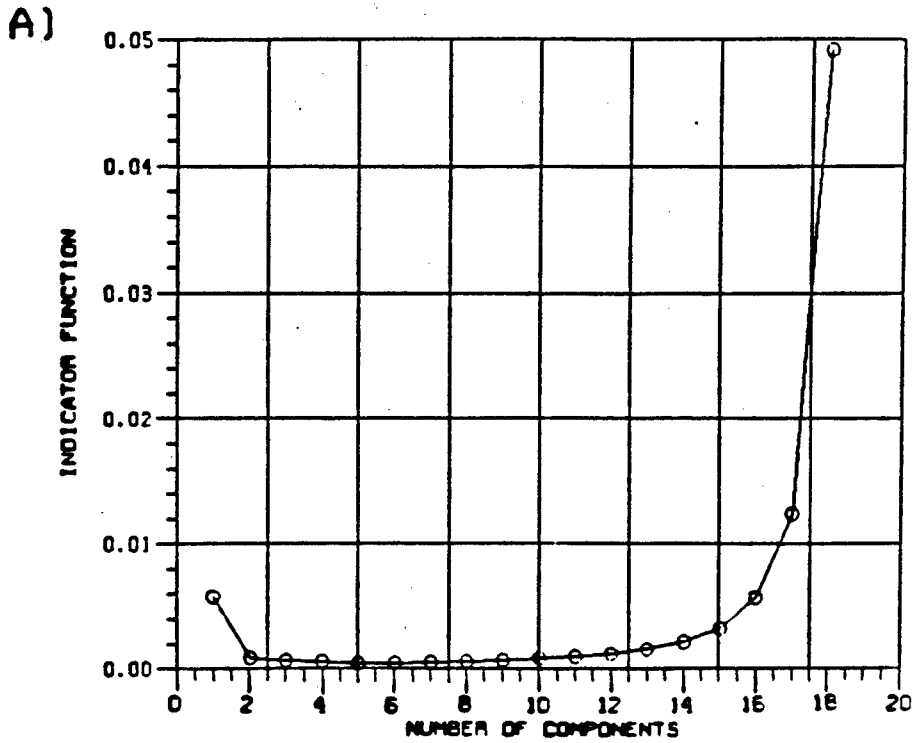


Figure 15. Indicator function vs. number of components calculated for mixture spectra of ATS cure at a) 150 C and b) 180 C.

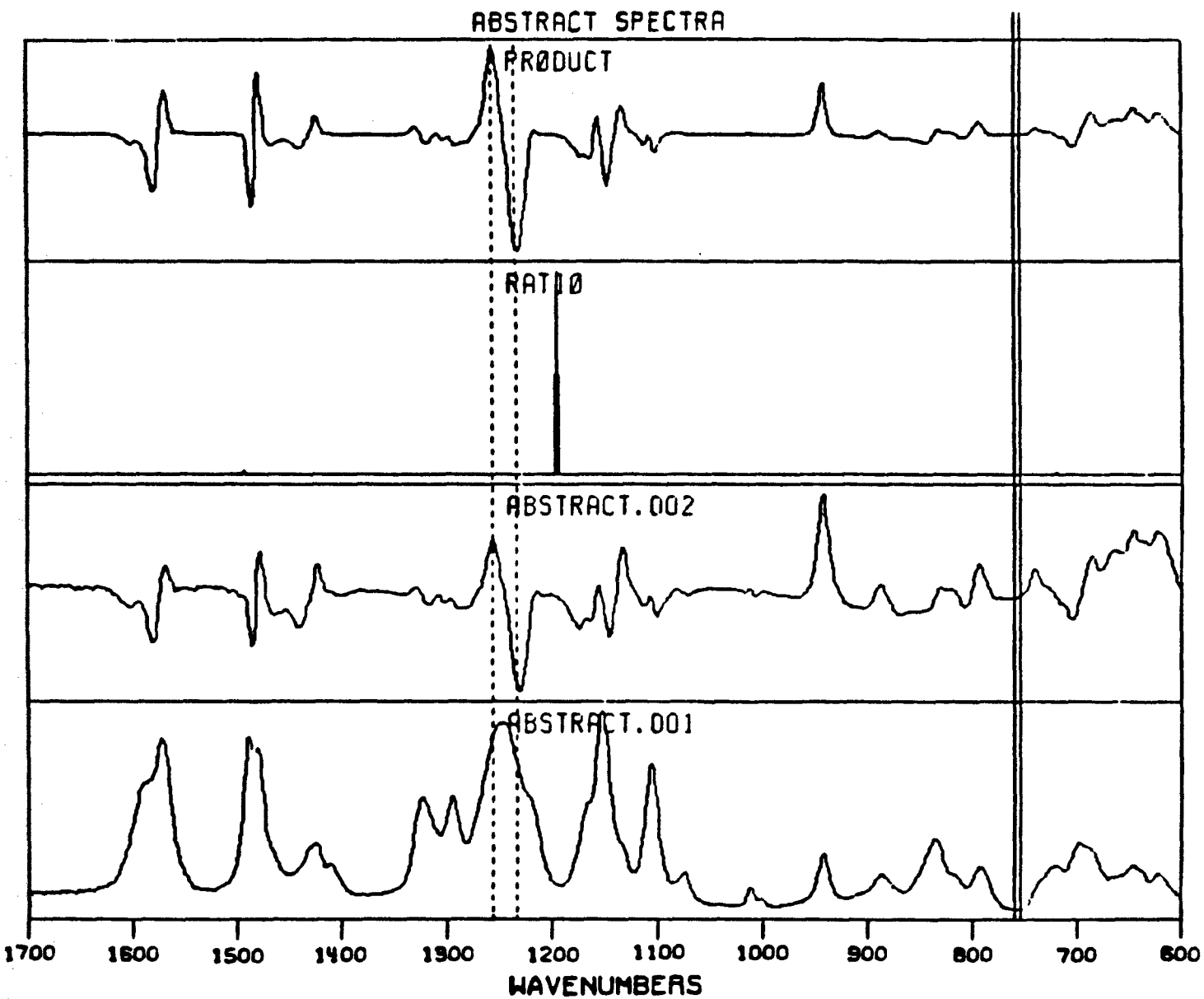


Figure 16. Regions of abstract spectra used to calculate pure component spectra for ATS cure at 150 C. Dotted lines indicate ratio region.

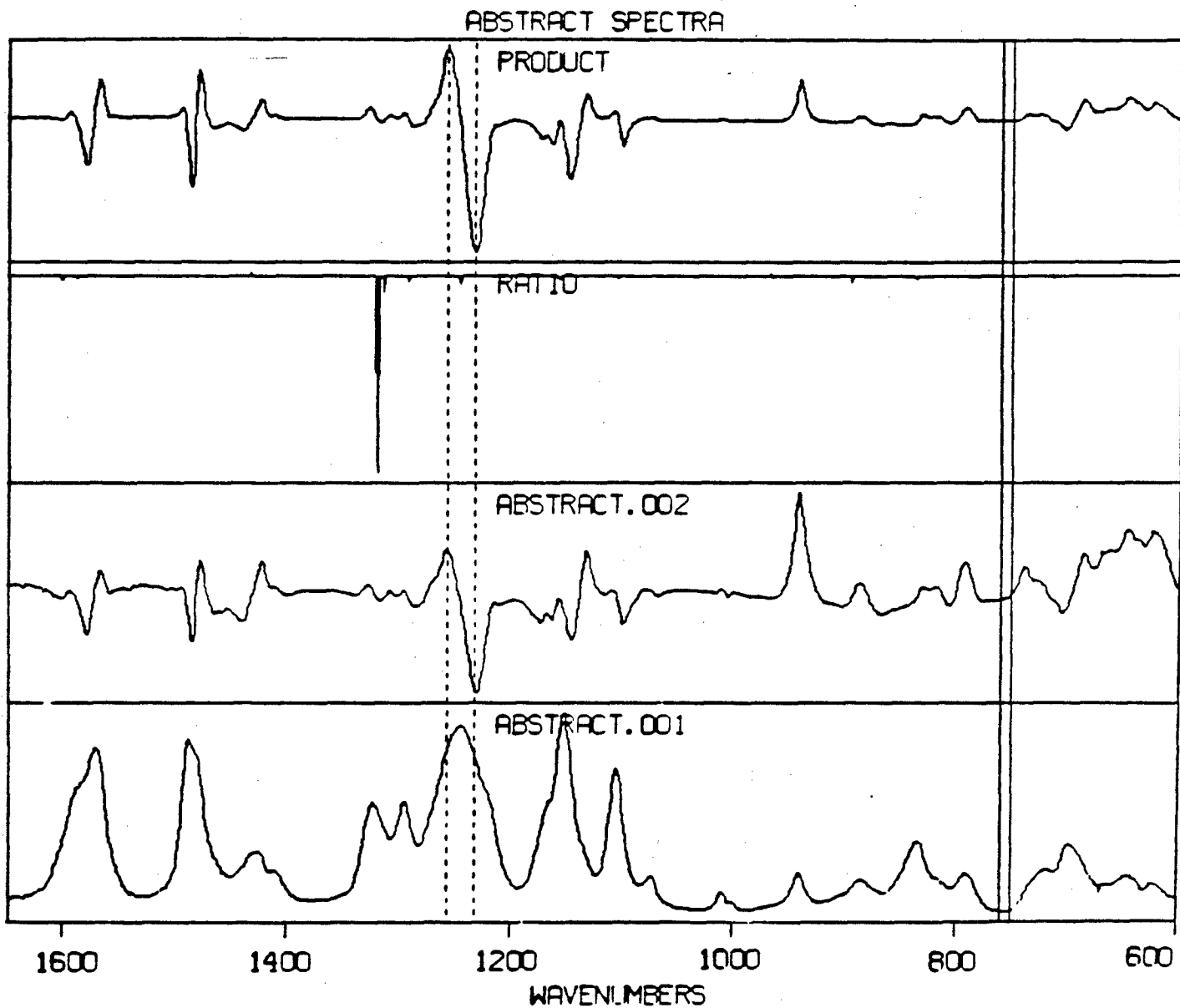
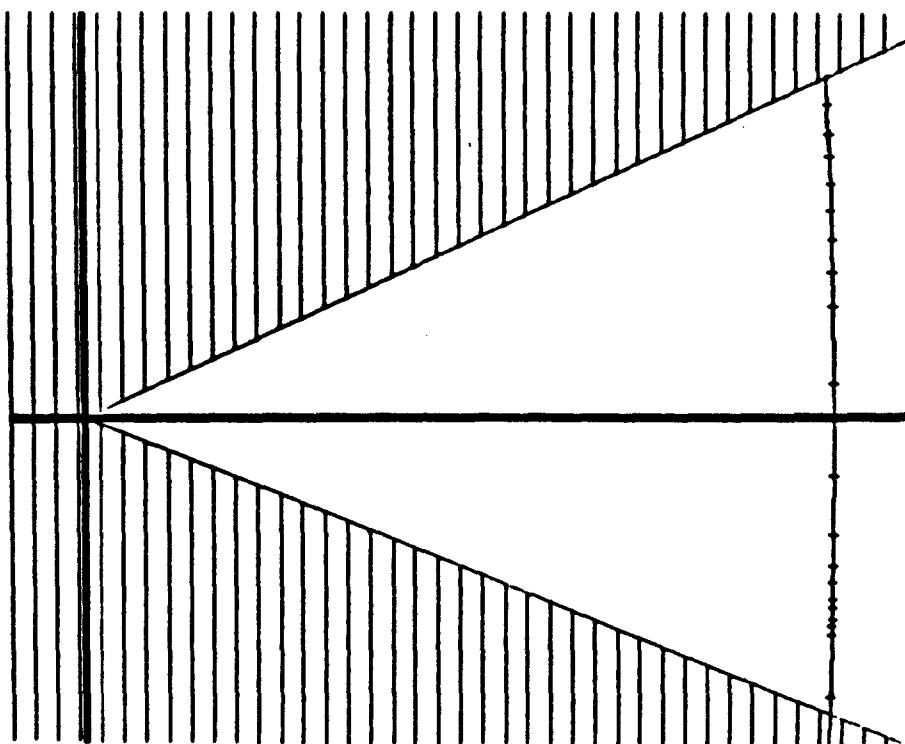


Figure 17. Regions of abstract spectra used to calculate pure component spectra for ATS cure at 180 C. Dotted lines indicate ratio region.

A)



B)

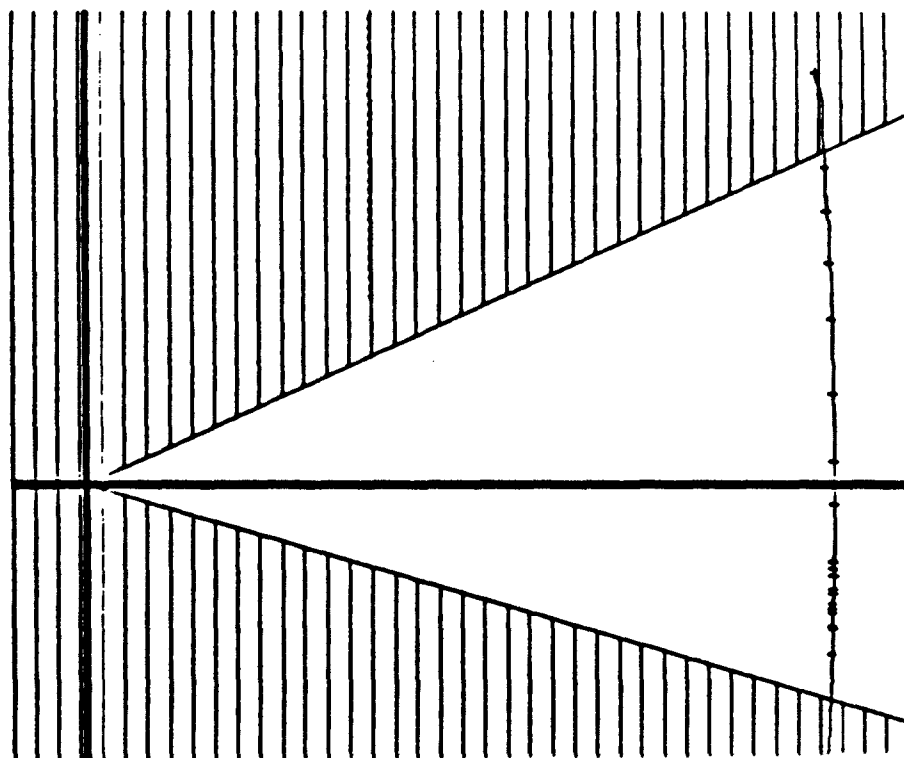


Figure 18. Plot of relative positions of mixture spectra and pure component spectra for ATS cure at a)150 C and b)180 C.

EXTRACTED PURE SPECTRA

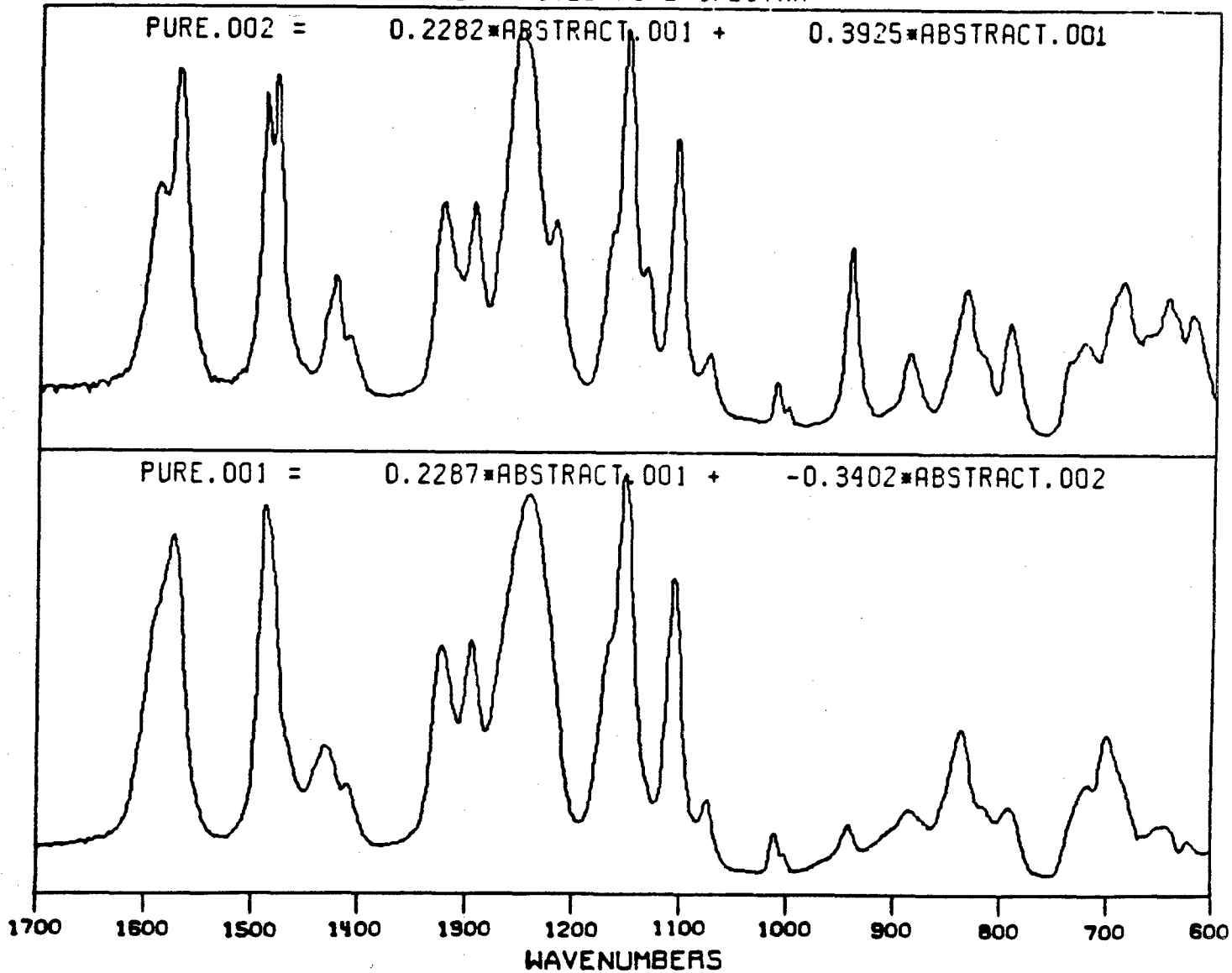
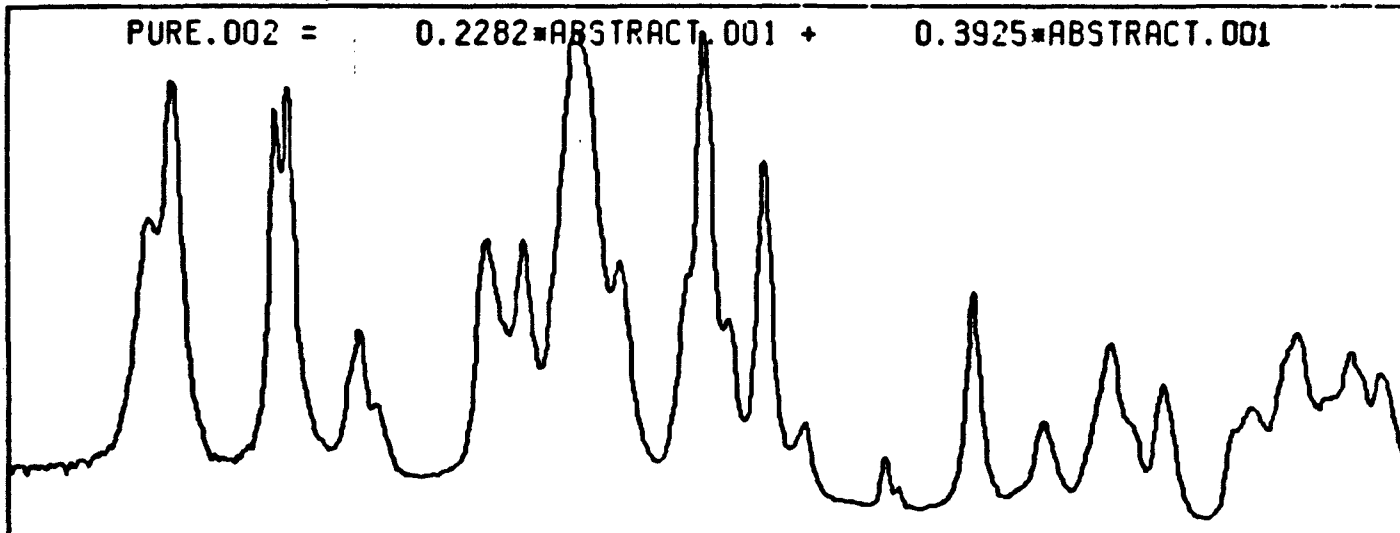


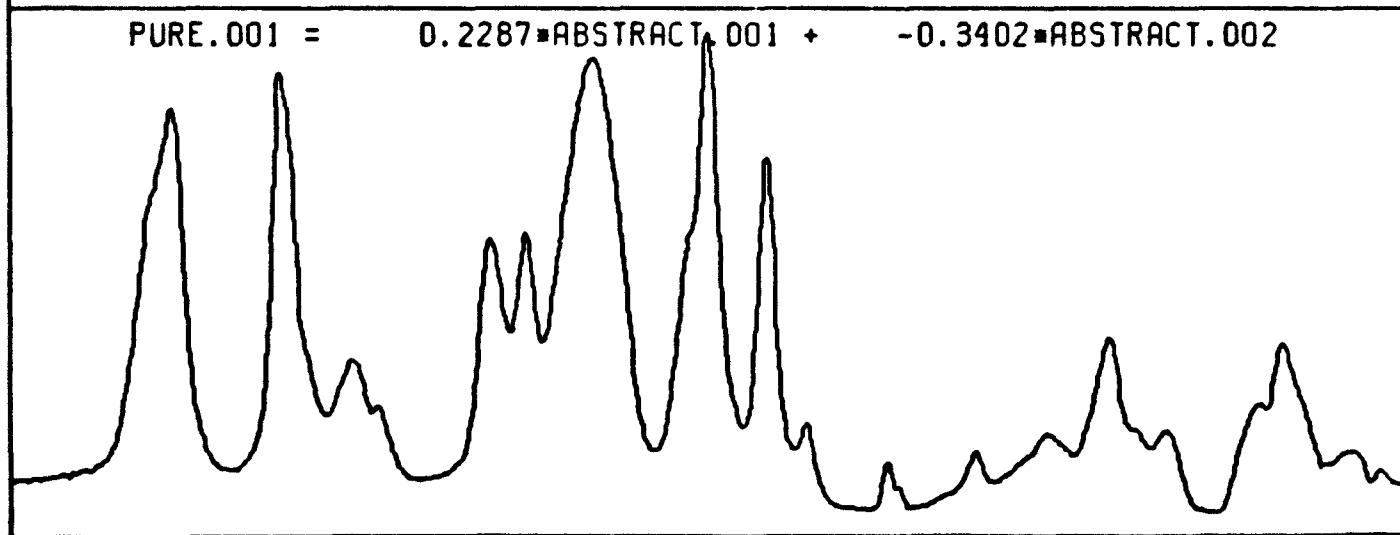
Figure 19. Calculated pure spectra from mixture spectra of ATS cure at 150 C.

EXTRACTED PURE SPECTRA

$$\text{PURE.002} = 0.2282 \cdot \text{ABSTRACT.001} + 0.3925 \cdot \text{ABSTRACT.001}$$



$$\text{PURE.001} = 0.2287 \cdot \text{ABSTRACT.001} - 0.3402 \cdot \text{ABSTRACT.002}$$



1700 1800 1500 1400 1300 1200 1100 1000 900 800 700 600
WAVENUMBERS

Figure 20. Calculated pure spectra from mixture spectra of ATS cure at 180 C.

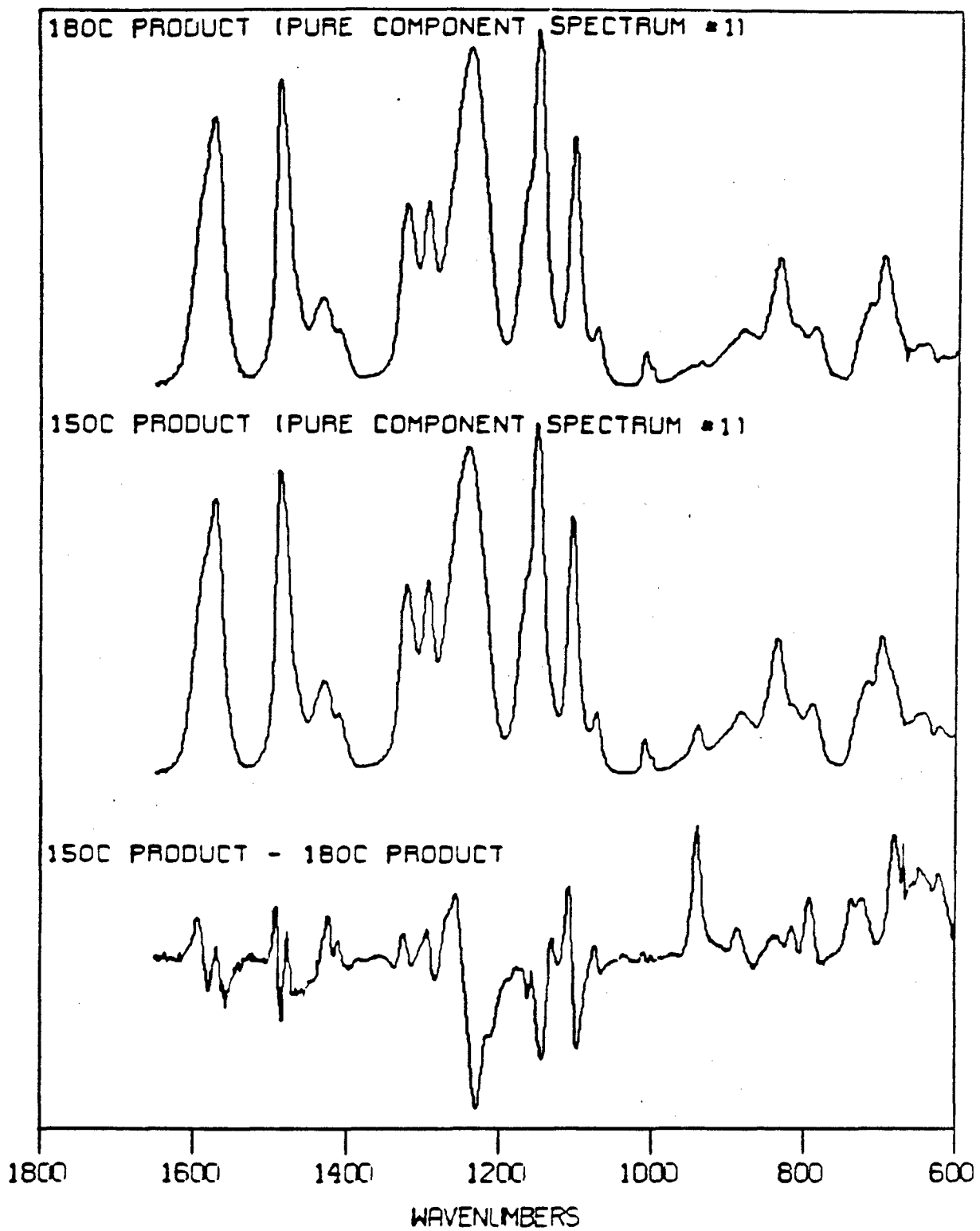


Figure 21. Difference spectra between pure components corresponding to products of ATS cure at 180 C and 150 C.

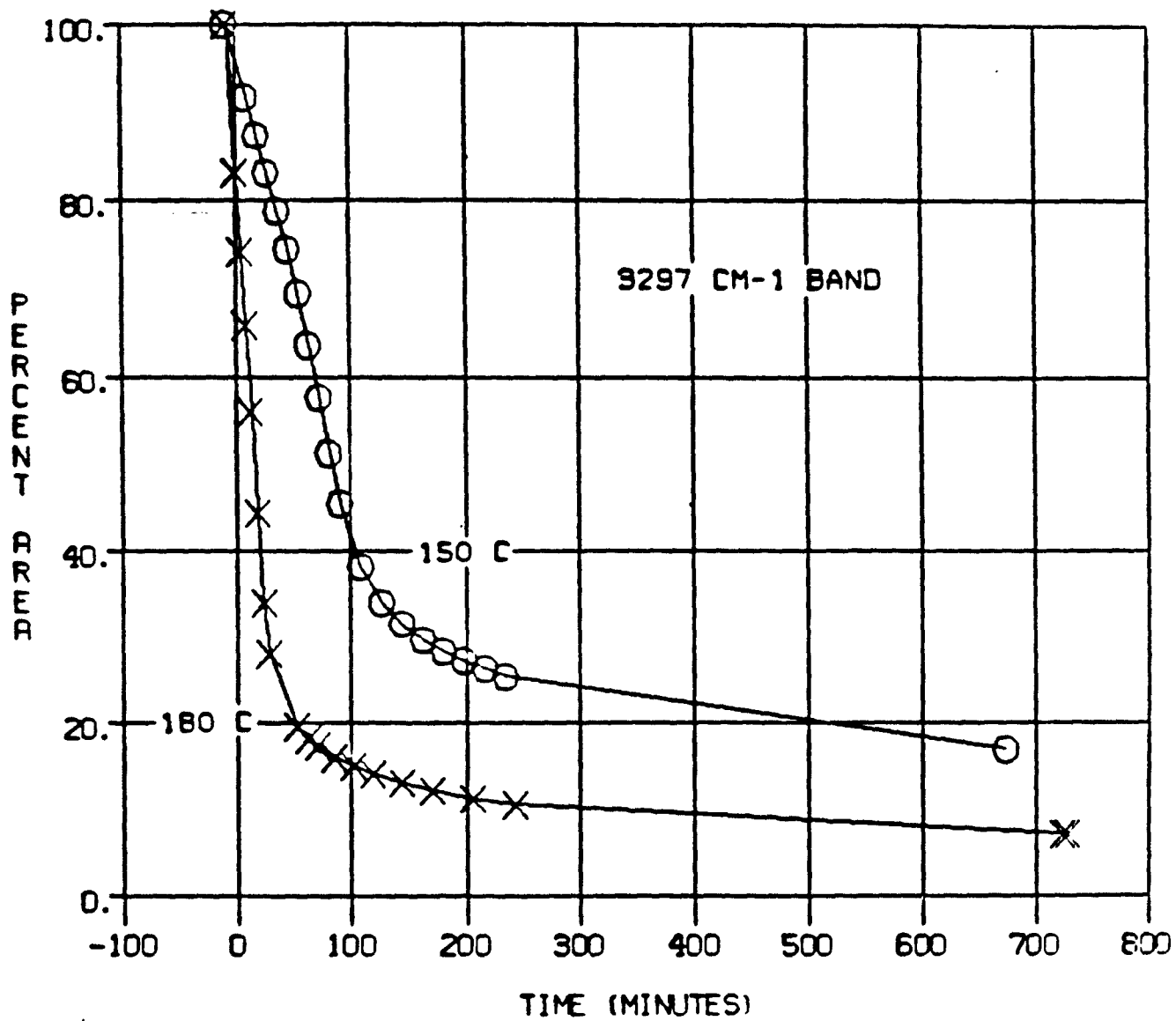


Figure 22. Percentage of acetylene loss as measured from band at 3300 cm^{-1} for ATS cure at 150 C and 180 C.

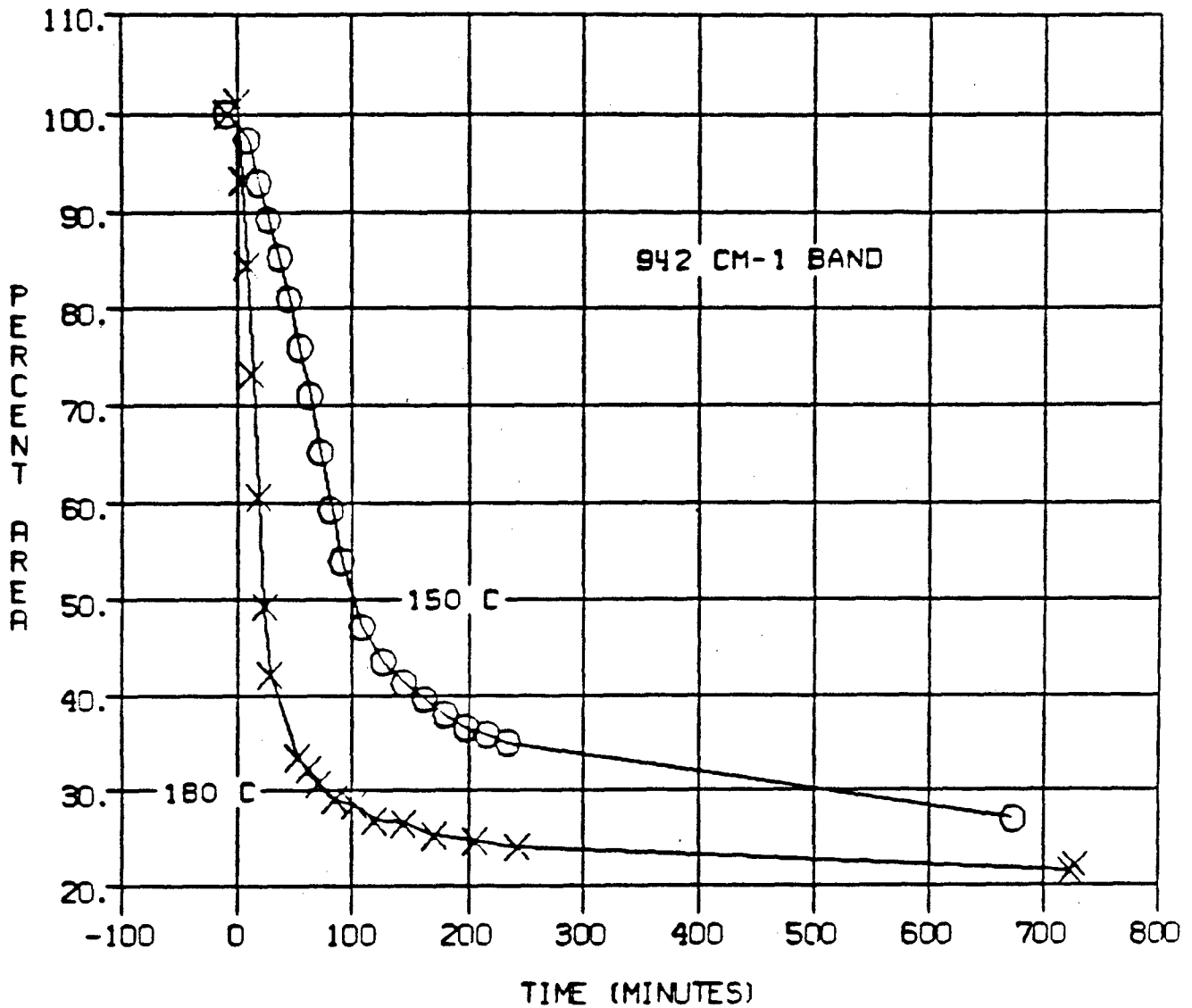


Figure 23. Percentage of acetylene loss as measured from band at 942 cm⁻¹ for ATS cure at 150 C and 180 C.

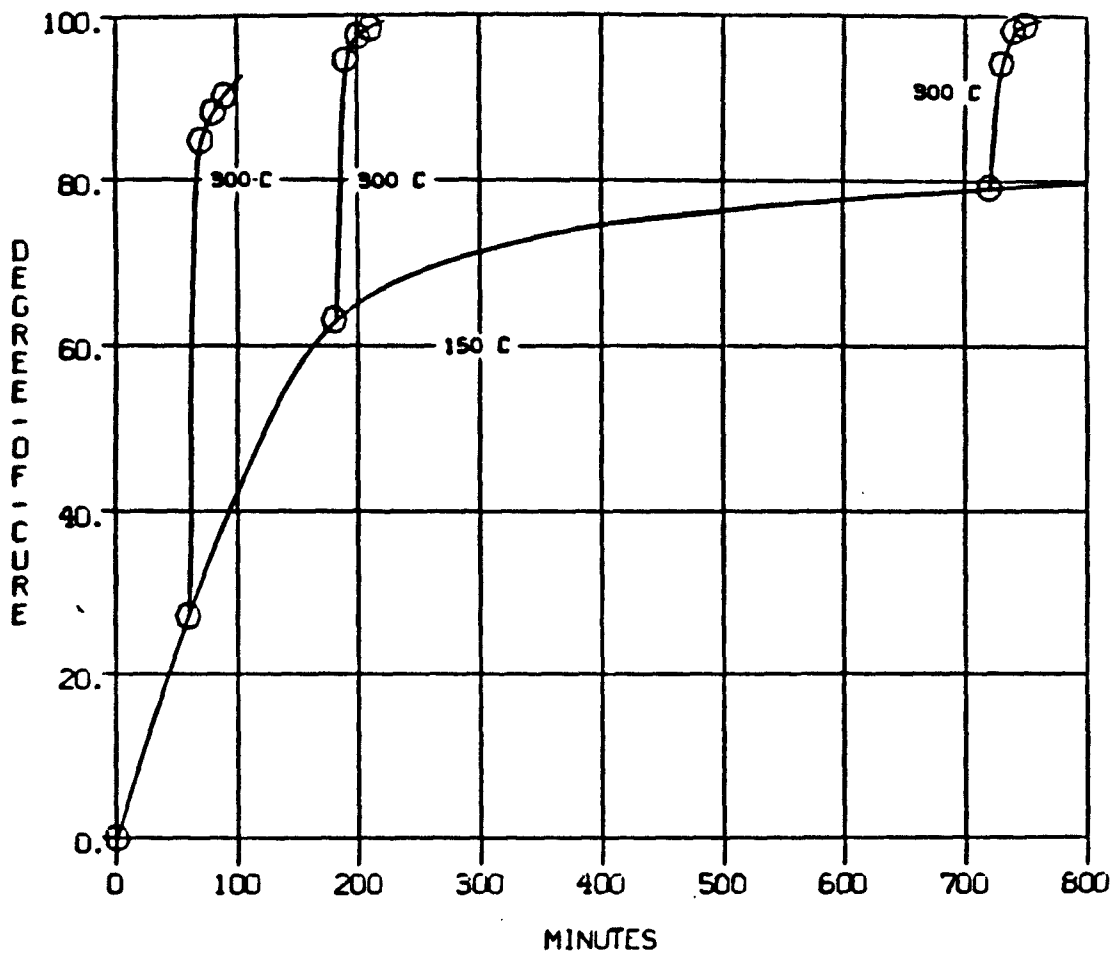


Figure 24. Degree of cure as measured from 3300 cm^{-1} band versus time of cure at 150 C and postcures at 300 C.

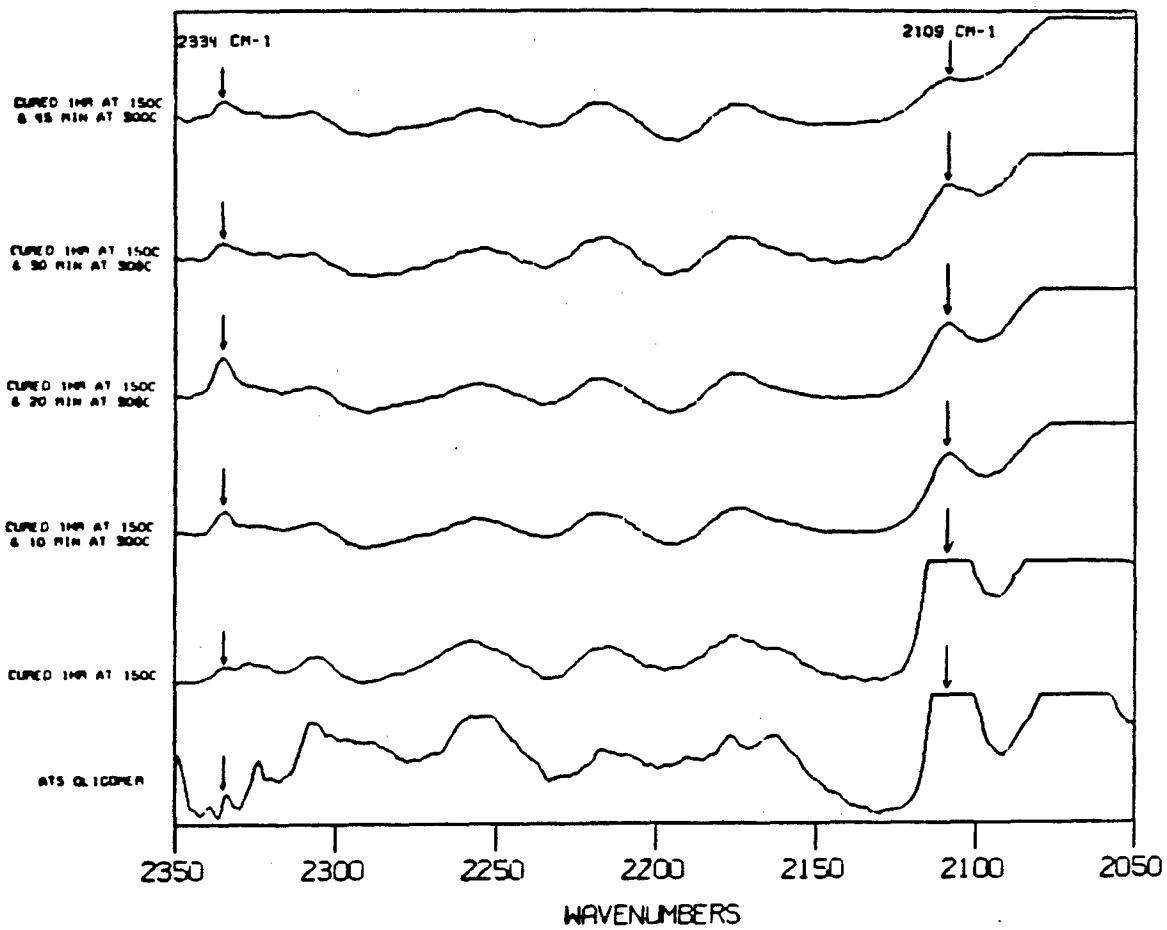


Figure 25. FTIR spectra of ATS cured 1 hr at 150 C and postcured for various times at 300 C.

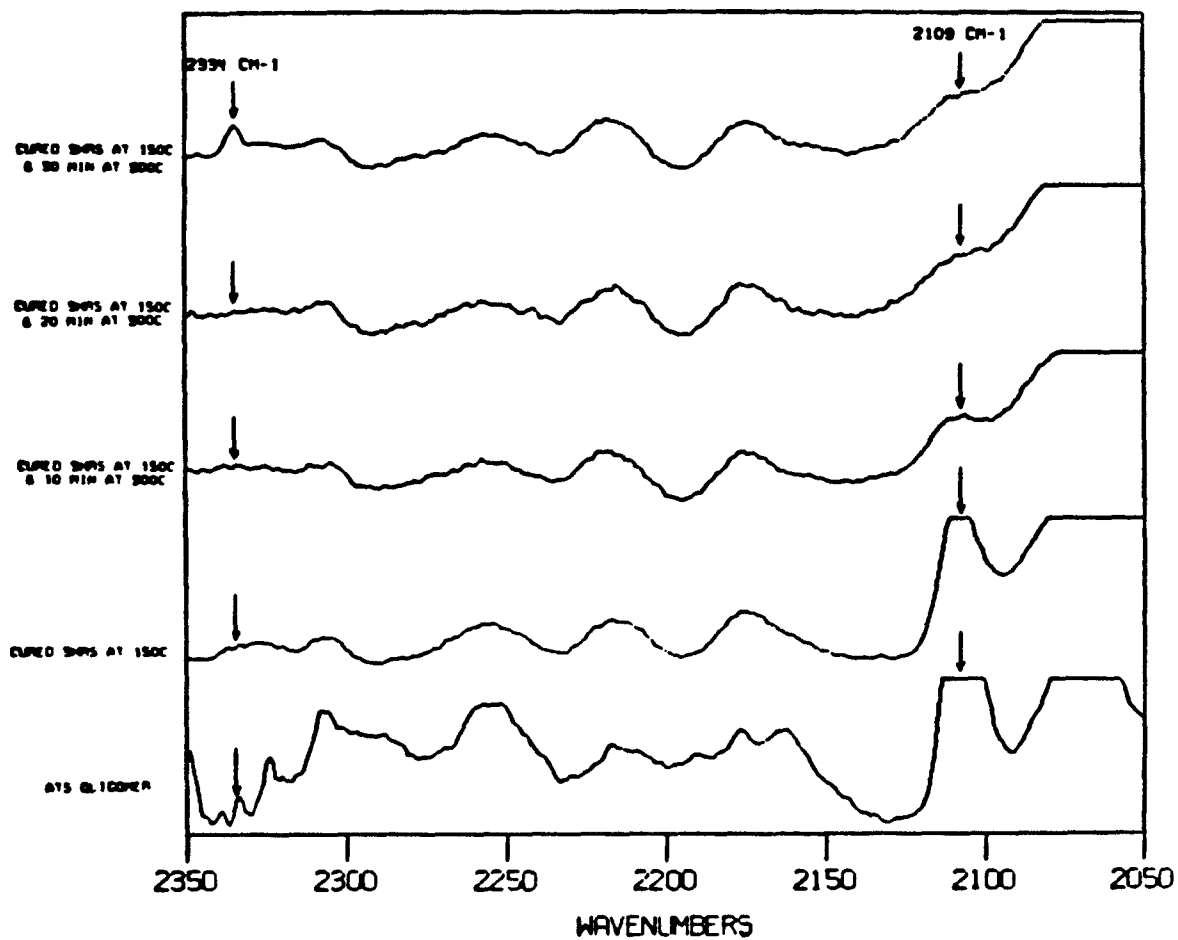


Figure 26. FTIR spectra of ATS cured 3 hrs at 150 C and postcured for various times at 300 C.

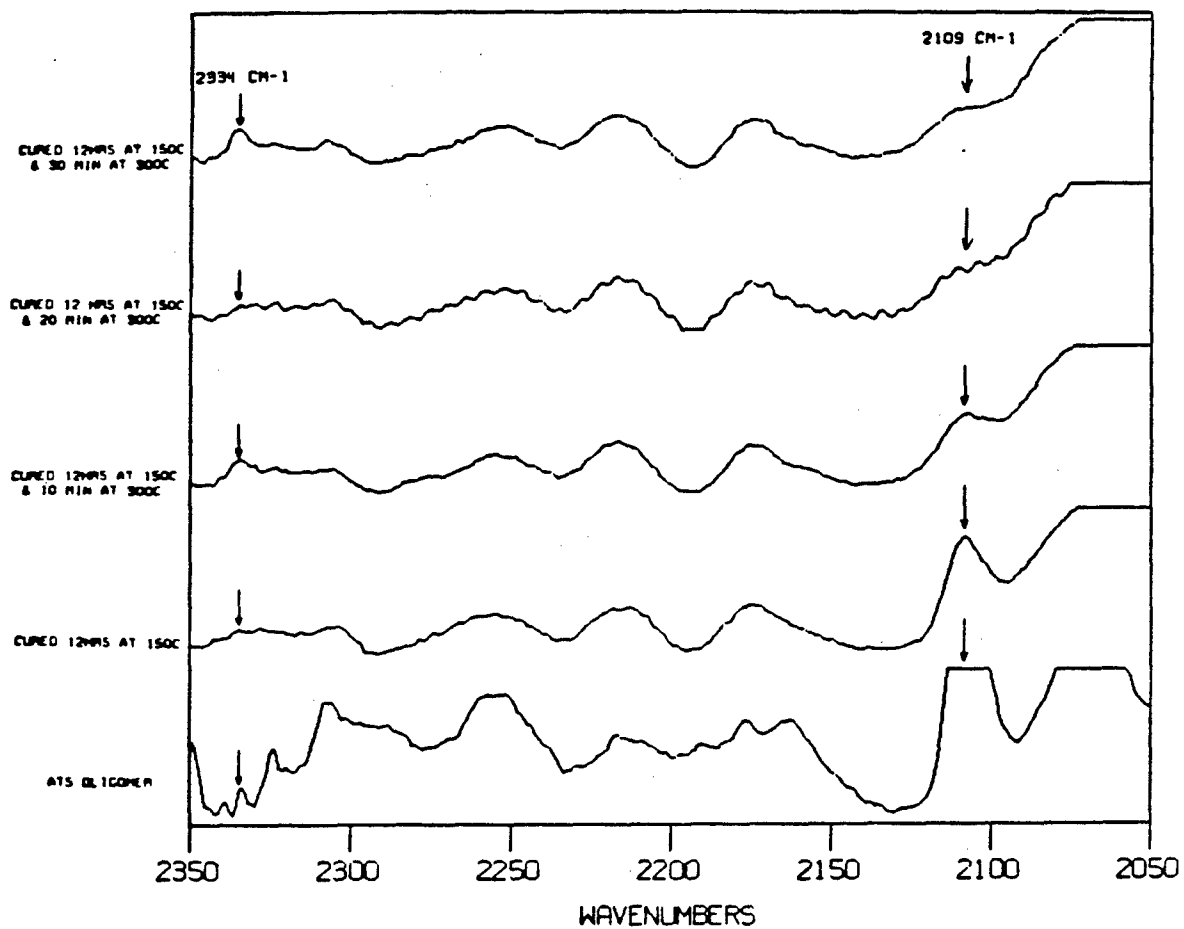


Figure 27. FTIR spectra of ATS cured 12 hrs at 150 C and postcured for various times at 300 C.

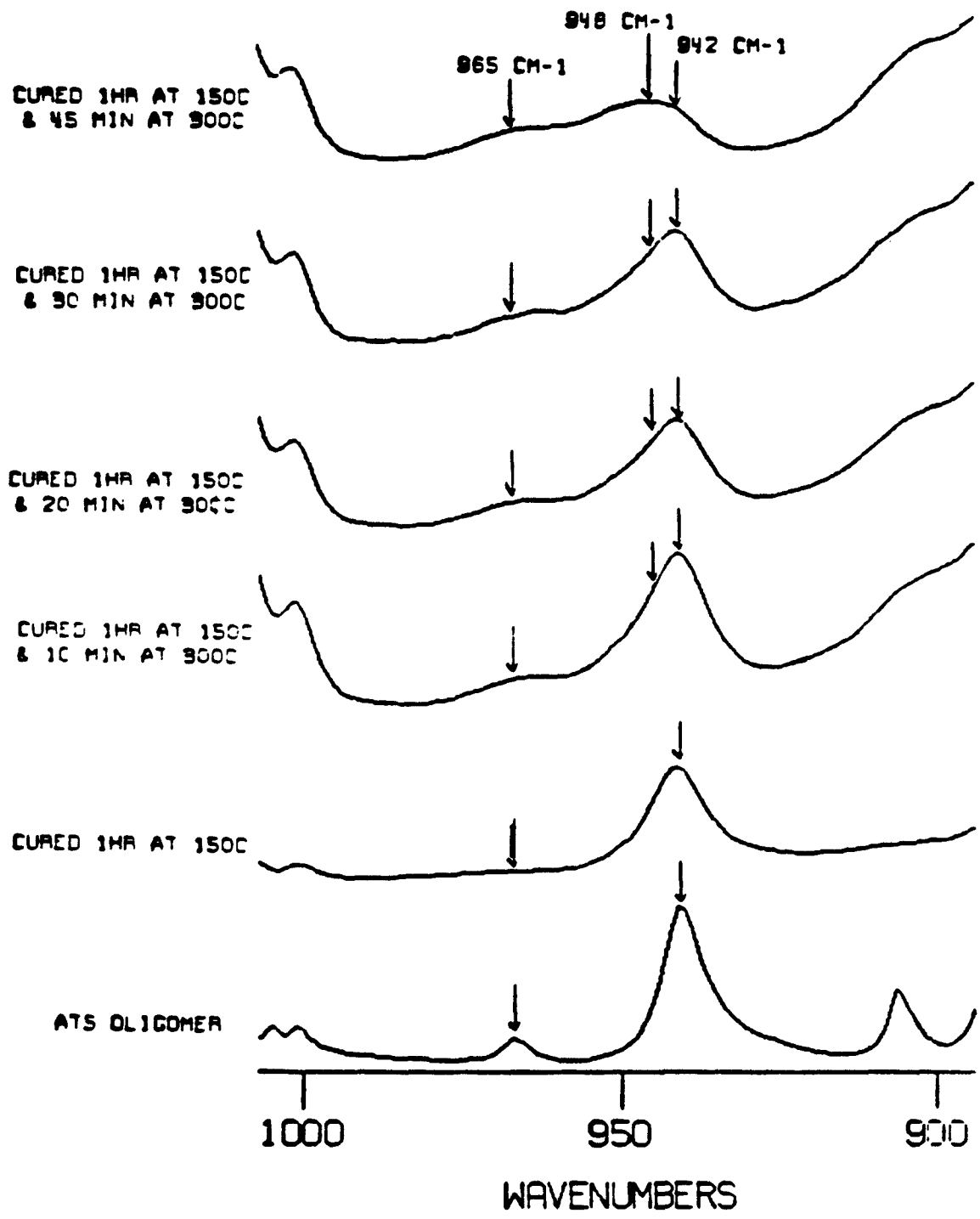


Figure 28. FTIR spectra of ATS cured 1 hr at 150 C and postcured for various times at 300 C.

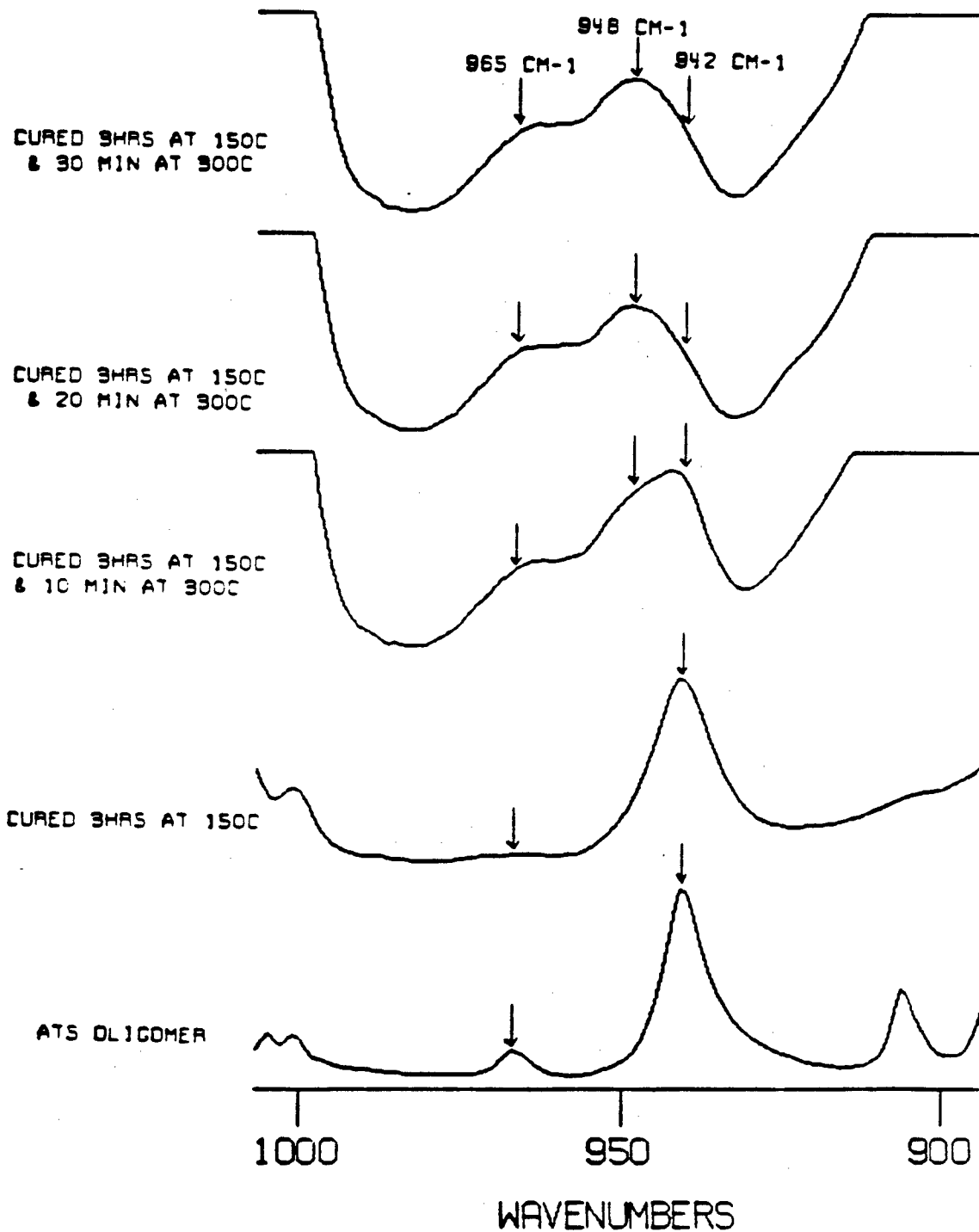


Figure 29. FTIR spectra of ATS cured 3 hrs at 150 C and postcured for various times at 300 C.

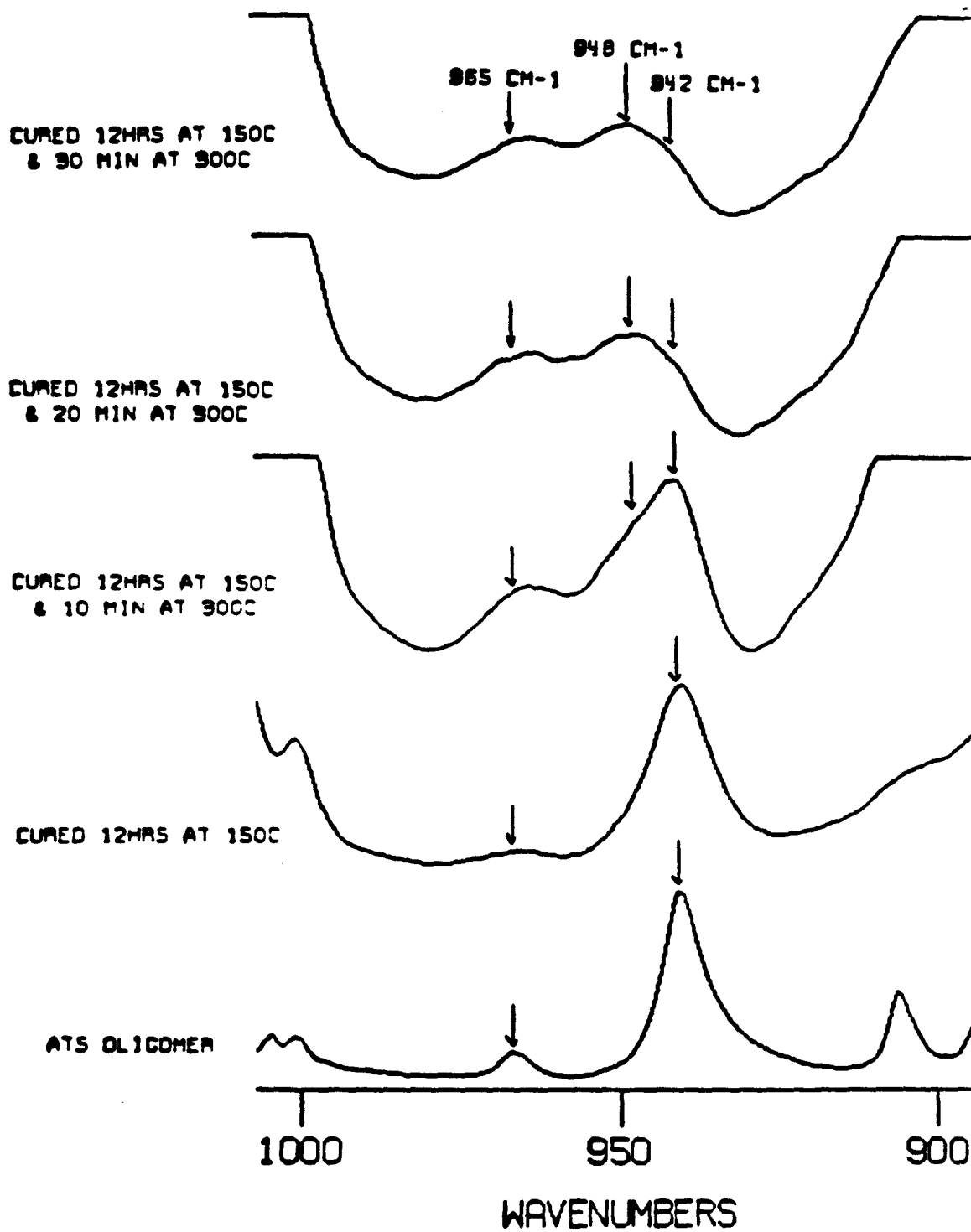


Figure 30. FTIR spectra of ATS cured 12 hrs at 150 C and postcured for various times at 300 C.